A complementary energy formulation of no tension masonry-like solids

Massimo Cuomo, Giulio Ventura

A complementary energy formulation of no tension masonry-like solids

M. Cuomo , G. Ventura

Facolta di Ingegneria, Istituto di Scienza delle Costruzioni, Universita di Catania, Viale A. Doria, 6, 95125 Catania, Italy

Abstract

In the present work a complementary energy formulation for the solution of the static equilibrium problem of no tension solids is presented. The main feature of the work is systematic use of the augmented Lagrangian approach for the regularisation of the nonsmooth and nondifferentiable anelastic deformation potential. The proposed formulation is applied to derive a finite element formulation using the subspace of the self equilibrated stresses as primal variables. The code implements the augmented Lagrangian algorithm for the determination of the inelastic deformations. Some numerical examples are included to illustrate the performance of the proposed approach.

1. Introduction

Among the methods of analysis of masonry structures a broad distinction can be made between approaches based on refined mechanical modeling of the elements constituting the masonry (e.g. mortar, stones or bricks, etc.), requiring a very large number of material parameters, and those based on homogenisation techniques. For many realistic cases a continuum idealization of stone and masonry structures can be based on a few simple hypotheses, that is, crushing of the material is not attained and crisis occurs due to crack openings and loss of the equilibrium state.

Many models have been proposed for the analysis of masonry that account for several phenomena such as cohesive cracks [1] energy release due to crack opening or dissipation due to interfacial crack friction etc. [2]. The no-tension material model is the simplest one that allows the brittle behaviour of the structure to be accounted for, at the cost of extreme idealization, that is, since the tensile strength is assumed to be zero, it is not possible to account for energy dissipation, and the response of the material turns out to be reversible, in a quite unrealistic way. However, the no-tension material model has received great attention by many authors, both because of its apparent simplicity although its numerical treatment is not trivial and because of its proved ability to approximate with reasonable accuracy the response of many important structures, such as stone block structures with poor or no binding, ancient masonries with diffuse cracking, etc. The no-tension model is especially useful for some particular structural typologies such as arches or for modelling mortar interfaces. Indeed, it was first employed on a scientific basis by Castigliano for the analysis of masonry arch bridges [3] and reproposed in the sixties in connection with masonry vaults [4].

In spite of the many objections that have been moved against the usefulness of the model (see, e.g., [8]) the authors believe that it is still of crucial importance in the static analysis of masonry structures, as a necessary reference solution, preliminary to the application of more sophisticated models which, because of their complexity, can lead to misleading solutions: first, the choice itself of an appropriate model depends not only on the material, but also on the nature of the problem being analysed; furthermore, the more complex the model is, the larger the number of parameters that need to be experimentally evaluated. However, it may be very difficult or even impossible to perform accurate estimations of the mechanical parameters on ancient and monumental masonries, both because of the infeasibility of destructive "in situ" tests, and because of the large variation in masonry typology within the same element that is often found in ancient structures. On the contrary, the no-tension model only requires knowledge of the elastic parameters, that can easily be obtained with standard nondestructive tests like flat jack tests.

The fundamental hypotheses on which the model relies are the existence of an elastic deformation potential, zero tensile strength, enforced by the requirement that the stress tensor be negative semidefinite, and normality between the stress and inelastic deformation fields. The no-tension material model has usually been analysed by introducing the hypothesis of small displacements and strains, consequently considering additivity for elastic and inelastic deformations. Four basic approaches are reported in literature:

- total displacement formulations [5,6];
- displacement rate formulations [7,8];
- stress (complementary) formulations with the linearisation of the admissible stress set to achieve a linear complementary problem [9];
- stress (complementary) formulations with no linearisation of the admissible stress set [10].

In the present work the hypothesis of small displacements is retained. In view of the nondissipative behaviour of the no-tension model the problem can be formulated in the total variables. For this reason a no-tension material is a generalised (conewise) elastic material according to the definition of Curnier et al. [11].

Although many authors have proposed computational formulations for no-tension materials, it is generally recognised that it is very difficult to achieve satisfactory efficiency in numerical implementations. It is well known that in many cases no solution exists, and when it does, it is often a discontinuous one. Indeed, in no-tension problems even if an equilibrated solution exists and is unique, the displacement field may be indeterminate or may diverge [14]. The main objectives of this work are twofold. First a variational formulation for the problem will be presented, based on a generalisation of the Hellinger–Reissner functional, eliminating the displacements from the functional by enforcing the equilibrium equations in a weak form and restating the problem on the set of self-equilibrated stresses only. This allows a significant reduction in the size of the problem while the displacements may be calculated once the solution for the stresses has been found. Secondly, the functional thus obtained — a nonregular one due to the presence of the admissibility constraints on the stress field — is consistently regularised using an augmented Lagrangian technique, that allows very efficient numerical solution methods to be employed. This technique has been previously used mainly for contact problems, where the number of constraints is much smaller than in the present case. The variational formulation proposed is implemented in an effective computational algorithm, which avoids most of the shortcomings usually found using displacement-based methods, as observed by Genna [8], without introducing approximations on the hypothesis of zero tensile stress.

In Section 2 of the paper the constitutive equation for the no-tension material is revisited, introducing the elastic and inelastic deformation potentials and their conjugate counterparts. These potentials are used to extend the Hellinger–Reissner variational principle to no-tension solids and a nondifferentiable mixed generalised variational principle is derived. From this functional a differentiable one is obtained by substituting the nondifferentiable inelastic strain potential with its augmented Lagrangian regularisation. The equivalence of the nonregular and regularised formulations is proved. Maximum principal stress and stress-invariant forms of the admissibility constraint are considered and their different properties are outlined.

In Section 3 the problem is solved numerically after discretising the stresses and the displacements on a finite element mesh and solving the nonlinear saddle point problem on the self-equilibrated stresses and discrete Lagrangian multipliers using an augmented Lagrangian iteration [26]. This allows a stable and efficient numerical implementation of the method to be obtained.

In the final section of the paper some numerical examples are used to illustrate the methodology proposed.

2. Variational formulation

2.1. Field variables

Let us consider a body occupying a region $\mathscr{B}$ and let $\partial\mathscr{B}$ be its boundary, partitioned into two disjoint parts, $\partial\mathscr{B}_u$ where the displacements u are prescribed, and $\partial\mathscr{B}_q$ where the surface loads q are applied. The volume forces applied in $\mathrm{Int}(\mathscr{B})$ (the internal part of $\mathscr{B}$) and the reactions on the constrained part $\partial\mathscr{B}_u$ of the body will be indicated by b and r.

The displacements u and the external forces f are elements of dual real linear vector spaces $\mathscr{V}_0$ and $\mathscr{V}_0'$,

$$\mathscr{V}_0 = \{u \in \mathscr{U} : u = 0 \text{ on } \partial\mathscr{B}_u\}. \tag{1}$$

Introducing the set $\mathscr{V}_1$ of the functions satisfying the nonhomogeneous boundary conditions

$$\mathscr{V}_1 = \{u \in \mathscr{U} : u = \overline{u} \text{ on } \partial\mathscr{B}_u\}, \tag{2}$$

the admissible displacement set $\mathscr{V}$ is given by the sum of the elements of $\mathscr{V}_0$ and an arbitrary element $\widehat{u} \in \mathscr{V}_1$:

$$u \in \mathscr{V} = \{u_0 + \widehat{u},\ u_0 \in \mathscr{V}_0\ \forall \widehat{u} \in \mathscr{V}_1\}. \tag{3}$$

The space $\mathscr{U}$ and its dual has been deeply investigated, from a mathematical point of view, in papers by Anzelotti [12], Giaquinta and Giusti [13] and Del Piero [14]. The authors gave different definitions of these spaces and the interested reader can find details on this subject in the relative papers. Here it is recalled that in general it is assumed that the displacement space $\mathscr{U}$ is contained in $BD(\mathscr{B})$, the set of all functions of the Sobolev space $\mathscr{L}^1(\mathscr{B})$ whose deformations are bounded measures. In [15] Del Piero developed a generalisation for the Gauss Green formula that can be used to supply a weak formulation of the equilibrium problem.

Calling the traces of u and f on the boundary $\partial\mathscr{B}$ w and r, respectively, and denoting by v the restriction of u to $\mathrm{Int}(\mathscr{B})$, by $\langle , \rangle_0$ the scalar product in $\mathscr{L}^2$, by $\langle , \rangle_{\partial\mathscr{B}}$ the duality pairing between traces, and by $\langle , \rangle_{\mathscr{V}}$ the duality pairing between $\mathscr{V}_0$ and $\mathscr{V}_0'$, the virtual work is

$$\begin{aligned}\langle u, f\rangle_{\mathscr{V}} &= \langle v, b\rangle_0 + \langle w, q\rangle_{\partial\mathscr{B}} + \langle w, r\rangle_{\partial\mathscr{B}} \\ &= \int_{\mathscr{B}} v \cdot b \,\mathrm{d}V + \int_{\partial\mathscr{B}_{q_d}} w \cdot q_d \,\mathrm{d}S + \mu \int_{\partial\mathscr{B}_{q_l}} w \cdot q_l \,\mathrm{d}S + \int_{\partial\mathscr{B}_u} w \cdot r \,\mathrm{d}S,\end{aligned} \tag{4}$$

$\cdot$ being the standard scalar product, i.e. $v \cdot b = v_i b_i$. In (4) the surface loads q are split into a permanent or "dead" part q_d and a part whose intensity is proportional to a scalar loading parameter μ. This distinction is useful especially in analysis of the incremental load problem.

The deformation tensor ε and the stress tensor σ are elements of the dual linear vector spaces $\mathscr{D}$ and $\mathscr{D}'$

$$\varepsilon \in \mathscr{D} = \{\text{symmetric second-order tensors on } \mathscr{R}^3 \text{ whose components are elements of } \mathscr{L}^2\}, \tag{5}$$

$$\sigma \in \mathscr{D}'. \tag{6}$$

The duality pairing between $\mathscr{D}$ and $\mathscr{D}'$ is defined by

$$\langle \varepsilon, \sigma\rangle_{\mathscr{D}} = \int_{\mathscr{B}} \varepsilon * \sigma \,\mathrm{d}V, \tag{7}$$

where $*$ is the standard inner product between tensors, given by

$$\varepsilon * \sigma = \varepsilon_{ij}\sigma_{ji} = \mathrm{tr}(\sigma^{\mathrm{T}}\varepsilon). \tag{8}$$

2.2. The no-tension material constitutive equation

The no-tension constitutive behaviour is founded on three physical hypotheses

(a) the material cannot resist any tensile stress;

(b) the strains can be decomposed into an elastic part and an inelastic one, due to crack openings that develop perpendicularly to the plane of maximum (nonnegative) stress;

(c) the material is elastic in compression.

From hypotheses (a) and (b) it follows that during the fracture process there is no dissipation of energy. Hypothesis (c) is not essential; however, in real situations compressive stresses are well below the elastic limit, so that inelastic phenomena can be neglected. These hypotheses can be formally expressed through the following assumptions

Assumption 1. The stress tensor must be negative semidefinite

$$\sigma \in \mathscr{K}_\sigma = \left\{ \sigma \in \mathscr{D}' : \sigma \text{ negative semidefinite} \right\}. \tag{9}$$

This assumption ensures the nonexistence of tensile principal stresses $(\sigma_1, \sigma_2, \sigma_3)$ and states that the admissible stress domain $\mathscr{K}_\sigma$ is a closed convex cone in the stress space $\mathscr{D}'$ (Fig. 1). If n is the generic normal at a point, from the definition of $\mathscr{K}_\sigma$ it follows that

$$\begin{aligned} \mathscr{K}_\sigma &= \left\{ \sigma \in \mathscr{D}' : \sigma n \cdot n \leqslant 0 \ \forall n \right\} \\ &= \left\{ \sigma \in \mathscr{D}' : \sigma_1 \leqslant 0, \sigma_2 \leqslant 0, \sigma_3 \leqslant 0 \right\}. \end{aligned} \tag{10}$$

Assumption 2. The total (infinitesimal) deformation field ε can be additively decomposed into an elastic part ε^{e} and an inelastic one ε^{a}

$$\varepsilon = \varepsilon^{\mathrm{e}} + \varepsilon^{\mathrm{a}}. \tag{11}$$

Because of hypothesis (b) the inelastic deformation tensor must be positive semidefinite

$$\varepsilon^{\mathrm{a}} \in \mathscr{K}_\varepsilon = \{ \varepsilon \in \mathscr{D} : \varepsilon \text{ positive semidefinite} \}. \tag{12}$$

It follows then that the scalar product between any two elements belonging to $\mathscr{K}_\sigma$ and $\mathscr{K}_\varepsilon$, respectively, is always nonpositive

$$\sigma * \varepsilon^{\mathrm{a}} \leqslant 0 \quad \forall \sigma \in \mathscr{K}_\sigma \ \forall \varepsilon^{\mathrm{a}} \in \mathscr{K}_\varepsilon \tag{13}$$

and that the scalar product of the inelastic deformation $\overline{\varepsilon}^{\mathrm{a}}$conjugate to a stress state $\overline{\sigma}$ is zero, i.e. the inelastic deformation is nondissipative

$$\overline{\sigma} * \overline{\varepsilon}^{\mathrm{a}} = 0 \quad \text{for any conjugate admissible pair } (\overline{\sigma}, \overline{\varepsilon}^{\mathrm{a}}). \tag{14}$$

From (13) and (14) it follows by subtraction that the inelastic deformation is such that

$$(\sigma - \overline{\sigma}) * \overline{\varepsilon}^{\mathrm{a}} \leqslant 0 \quad \forall \sigma \in \mathscr{K}_\sigma \ \ \forall (\overline{\sigma}, \overline{\varepsilon}^{\mathrm{a}}) \text{ conjugate admissible pair.} \tag{15}$$

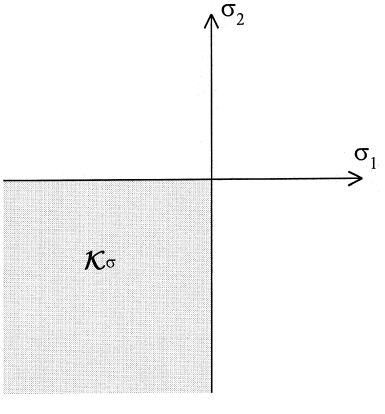

Fig. 1. The admissible stress space in two dimensions.

Inequality (15) is satisfied, by definition, by all the deformations belonging to $\mathscr{N}_{\mathscr{K}_\sigma}(\overline{\sigma})$, the outward normal cone to $\mathscr{K}_\sigma$ at the point $\overline{\sigma}$. The constitutive equation for inelastic deformation can be reformulated as

$$\varepsilon^{\mathrm{a}} \in \mathscr{N}_{\mathscr{K}_\sigma}(\overline{\sigma}) = \partial \operatorname{ind}_{\mathscr{K}_\sigma}(\overline{\sigma}). \tag{16}$$

In (14) ∂ denotes the subdifferential set and the function $\operatorname{ind}_{\mathscr{K}_\sigma}(\sigma)$ is equal to zero if $\sigma \in \mathscr{K}_\sigma$ and is equal to $+\infty$ otherwise.

Eq. (15) has the same form as the maximum dissipation postulate in plasticity with total deformations in place of rates, and is equivalent to the so-called hypothesis of normality to the boundary of the admissible stress domain $\mathscr{K}_\sigma$ (Fig. 2).

From (14) it is observed that in a no-tension material the conjugate pair $(\sigma, \varepsilon^{\mathrm{a}})$ is orthogonal and that the stress and inelastic deformation tensors have the same principal directions. Expressing (14) in the principal reference system the following Kuhn Tucker optimality conditions are obtained

$$\sigma_i \varepsilon_i^{\mathrm{a}} = 0, \quad \sigma_i \leqslant 0, \quad \varepsilon_i^{\mathrm{a}} \geqslant 0 \quad i = 1 \ldots 3 \text{ (no sum on } i). \tag{17}$$

The no-tension constitutive law can be derived following an alternate path. Note, in fact, that it is possible to define a work functional D analogous to the dissipated power functional in elastoplasticity

$$D(\varepsilon^{\mathrm{a}}) = \operatorname{ind}_{\mathscr{K}_\varepsilon}(\varepsilon^{\mathrm{a}}) \Longleftrightarrow \varepsilon^{\mathrm{a}} \in \mathscr{K}_\varepsilon, \quad \overline{\sigma} * \overline{\varepsilon}^{\mathrm{a}} = 0 \quad \forall(\overline{\sigma}, \overline{\varepsilon}^{\mathrm{a}}), \tag{18}$$

$(\overline{\sigma}, \overline{\varepsilon}^{\mathrm{a}})$ being a conjugate admissible pair. Since

$$\operatorname{ind}_{\mathscr{K}_\varepsilon}(\varepsilon^{\mathrm{a}}) = \sup_{\sigma \in \mathscr{K}_\varepsilon^0} \sigma * \varepsilon^{\mathrm{a}}, \tag{19}$$

where $\mathscr{K}_\varepsilon^0$ is the polar cone to $\mathscr{K}_\varepsilon$, coincident with $\mathscr{K}_\sigma$ by definition, the following formulation of the maximum dissipation postulate (15) is obtained

$$D(\varepsilon^{\mathrm{a}}) = \sup_{\sigma \in \mathscr{K}_\sigma} \sigma * \varepsilon^{\mathrm{a}} = \operatorname{supp}_{\mathscr{K}_\sigma}(\varepsilon^{\mathrm{a}}). \tag{20}$$

Eq. (20) states that the dissipation functional $D(\varepsilon^{\mathrm{a}})$ is a potential whose conjugate is

$$D'(\sigma) = \operatorname{ind}_{\mathscr{K}_\sigma}(\sigma) \tag{21}$$

and the constitutive equations are therefore

$$\varepsilon^{\mathrm{a}} \in \partial D'(\sigma) = \partial \operatorname{ind}_{\mathscr{K}_\sigma}(\sigma), \tag{22}$$

$$\sigma \in \partial D(\varepsilon^{\mathrm{a}}) = \partial \operatorname{supp}_{\mathscr{K}_\sigma}(\varepsilon^{\mathrm{a}}). \tag{23}$$

This latter path is especially useful when some dissipation mechanism, such as damage or plasticity, is to be introduced into the formulation of the constitutive law. Furthermore, Eqs. (22) and (23) allow the present formulation to be placed within the framework of unilateral mechanics, so that the results obtained in that field can easily be extended to the problem at hand.

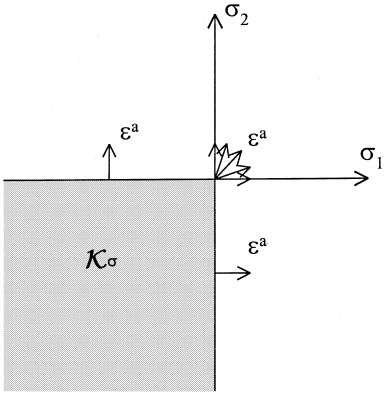

Fig. 2. Normality hypothesis in two dimensions.

Assumption 3. There exists a convex lower semicontinuous (l.s.c.) elastic potential whose complementary form $\phi^{\mathrm{e}}(\sigma)$ is such that

$$\varepsilon^{\mathrm{e}} = \partial\phi^{\mathrm{e}}(\sigma). \tag{24}$$

Since from (16) the inelastic complementary potential is given by $\phi^{\mathrm{a}}(\sigma) = \mathrm{ind}_{\mathscr{K}_\sigma}(\sigma)$, from Eq. (11) the total stress potential is

$$\phi(\sigma) = \phi^{\mathrm{e}}(\sigma) + \phi^{\mathrm{a}}(\sigma). \tag{25}$$

In fact, since $\phi^{\mathrm{a}}(\sigma)$ is continuous throughout its proper domain, and $\mathrm{dom}(\phi^{\mathrm{e}}) \cap \mathrm{dom}(\phi^{\mathrm{a}}) \neq \emptyset$ it turns out that $\partial(\phi^{\mathrm{e}} + \phi^{\mathrm{a}}) = \partial\phi^{\mathrm{e}} + \partial\phi^{\mathrm{a}}$. The potential $\phi(\sigma)$ is convex and l.s.c. and the no-tension material model under assumptions 1 ... 3 is therefore a generalized elastic material in the sense indicated by Curnier et al. [11].

If the elastic potential is the linear elastic one and E is the elastic operator, then

$$\phi^{\mathrm{e}}(\sigma) = \tfrac{1}{2}E^{-1}\sigma * \sigma. \tag{26}$$

In this particular case the deformation is given by the equations

$$\varepsilon^{\mathrm{e}} = E^{-1}\sigma, \quad \sigma \in \mathscr{K}_\sigma, \tag{27}$$

$$\varepsilon^{\mathrm{a}} \in \partial\,\mathrm{ind}_{\mathscr{K}_\sigma}. \tag{28}$$

Once the local potential $\phi(\sigma)$ is defined, the complementary deformation energy for the whole body is given by its Lebesgue integral

$$\Phi(\sigma) = \int_{\mathscr{B}} \phi(\sigma)\,\mathrm{d}V. \tag{29}$$

2.3. Equilibrium and compatibility equations

Throughout this work the assumption of infinitesimal deformation is retained. The compatibility and equilibrium equations can therefore be expressed by a linear operator $C : \mathscr{V}_0 \to \mathscr{D}$ and its adjoint $C' : \mathscr{D}' \to \mathscr{V}_0'$ in the form

$$Cu = \varepsilon = \varepsilon^{\mathrm{e}} + \varepsilon^{\mathrm{a}} \quad \text{in } \mathscr{B}, \tag{30}$$

$$C'\sigma = f \quad \text{in } \mathscr{B} \cup \partial\mathscr{B}_q. \tag{31}$$

In the following it will be assumed that

$$C = \mathrm{symgrad}; \quad C' = \begin{cases} -\mathrm{div} & \text{in } \mathscr{B}, \\ P & \text{on}, \end{cases} \tag{32}$$

where P is the mapping that gives the stress vector at a point on the surface of the body, i.e. if n denotes the outward unit normal at a point, $P\sigma = \sigma n$.

The structural problem defined by (30), (31), (16) and (24) admits a solution if and only if the applied forces are compatible, that is, if their virtual work is nonpositive for any virtual displacement field producing only admissible inelastic deformations [6]

$$f \text{ compatible} \iff \langle u, f\rangle_{\mathscr{V}} \leqslant 0 \quad \forall u \in \mathscr{V} : Cu \in \mathscr{K}_\varepsilon. \tag{33}$$

This condition stems from the statement that a solution exists if it is possible to find at least one stress field σ satisfying both the equilibrium equations and the admissibility condition (9) in $\mathscr{B}$, i.e. if the intersection of the set of equilibrated stress fields

$$\begin{aligned} \mathscr{K}_{\mathrm{e}} &= \left\{\sigma \in \mathscr{D}' : -\mathrm{div}\sigma = b \text{ in } \mathscr{B},\ P\sigma = q_{\mathrm{d}} + \mu q_{\mathrm{l}} \text{ on } \partial\mathscr{B}_q\right\} \\ &= \left\{\sigma \in \mathscr{D}' : C'\sigma = f\right\} \end{aligned} \tag{34}$$

and of the set of admissible stress fields $\mathscr{K}_\sigma$ is nonempty, $\mathscr{K}_{\mathrm{e}} \cap \mathscr{K}_\sigma \neq \emptyset$.

Other load compatibility conditions regarding the resultant and the moments over parts of the solid bounded by planar surfaces are reported in literature [16,17] and they allow the load compatibility in simple cases to be immediately assessed.

2.4. Variational principles — nondifferentiable form

In [6] extensions of the variational principles in elastostatics to the case of generalized elasticity were given. The solution of the structural problem represented by Eqs. (30), (31), (16), (24) and the relevant kinematic boundary conditions can be obtained as the saddle point of the following generalized Reissner functional, concave on σ, linear on $u$and defined in $\mathscr{V} \times \mathscr{D}'$

$$\Pi_{\mathrm{R}}(\sigma, u) = -\Phi(\sigma) + \langle \sigma, Cv \rangle_{\mathscr{D}} - \langle b, v \rangle_0 - \langle q_{\mathrm{d}}, w \rangle_{\partial \mathscr{B}_q} - \mu \langle q_{\mathrm{l}}, w \rangle_{\partial \mathscr{B}_q}. \tag{35}$$

The first Euler–Lagrange equation of Π_{R}, obtained by equating its first variation to zero w.r.t. the variable σ, yields the weak form of the kinematic compatibility equation (30)

$$\langle \sigma, Cv \rangle_{\mathscr{D}} = \langle \sigma, \varepsilon \rangle_{\mathscr{D}} \quad \forall \sigma \in \mathscr{D}' \qquad \text{subject to } \varepsilon \in \partial\phi(\sigma) = \partial\phi^{\mathrm{e}}(\sigma) + \partial\phi^{\mathrm{a}}(\sigma). \tag{36}$$

Integrating by parts the term $\langle \sigma, Cv \rangle_{\mathscr{D}}$ in (35) the functional becomes

$$\begin{aligned} \Pi_{\mathrm{R}}(\sigma, u) &= -\Phi(\sigma) + \left\langle C'\sigma, v \right\rangle_0 + \langle P\sigma, w \rangle_{\partial \mathscr{B}} - \langle b, v \rangle_0 - \langle q_{\mathrm{d}}, w \rangle_{\partial \mathscr{B}_q} - \mu \langle q_{\mathrm{l}}, w \rangle_{\partial \mathscr{B}_q} \\ &= -\Phi(\sigma) + \left\langle C'\sigma - b, v \right\rangle_0 + \langle r, \overline{u} \rangle_{\partial \mathscr{B}_u} + \langle P\sigma - q_{\mathrm{d}} - \mu q_{\mathrm{l}}, w \rangle_{\partial \mathscr{B}_q}, \end{aligned} \tag{37}$$

$r = P\sigma$ being the constraint reactions on $\partial\mathscr{B}_u$. The variation of (37) w.r.t. u yields the weak form of the equilibrium condition (31) as a second Euler–Lagrange equation of the Reissner functional

$$\left\langle C'\sigma, v \right\rangle_0 + \langle P\sigma, w \rangle_{\partial \mathscr{B}_q} = \langle b, v \rangle_0 + \langle q_{\mathrm{d}} + \mu q_{\mathrm{l}}, w \rangle_{\partial \mathscr{B}_q} \quad \forall u \in \mathscr{V}. \tag{38}$$

Under the hypothesis of load compatibility (33) the solution of the structural problem is given by the saddle point of (35)

$$\sup_{\sigma \in \mathscr{D}'} \operatorname{stat}_{u \in \mathscr{V}} \Pi_{\mathrm{R}}(\sigma, u). \tag{39}$$

The solution of the structural problem is also determined by the maximum of the complementary energy functional $\Pi_{\mathrm{C}}(\sigma)$ stemming from (37) when the weak form of the equilibrium equations (38) is satisfied

$$\Pi_{\mathrm{C}}(\sigma) = -\Phi(\sigma) + \langle r, \overline{u} \rangle_{\partial \mathscr{B}_u} \qquad \sigma \in \mathscr{K}_{\mathrm{e}}. \tag{40}$$

The functional (40) is the complementary energy functional generalized to no-tension solids and differs from the classical one by the presence of the term $\int_{\mathscr{B}} \mathrm{ind}_{\mathscr{K}_\sigma} \mathrm{d}V$ in the complementary deformation energy $\Phi(\sigma)$. The subsidiary conditions are given by the domain of definition of the independent variables.

Anzelotti [12] and Giaquinta and Giusti [13] studied the complementary energy functional and the total potential energy functional for no-tension solids and in their papers the following properties are proved:

- The total potential energy (TPE) functional is convex and l.s.c. and its coercivity depends on the applied loads (i.e. load compatibility is equivalent to inducing TPE coercivity). It is not strictly convex,
- The complementary energy (CE) functional is strictly concave and coercive, provided that loads are compatible.

Therefore, if the loads are compatible there exists a minimum $\tilde{u}$ of the TPE functional that represents the solution of the problem, but it is in general nonunique. From $\tilde{u}$ a unique stress field $\tilde{\sigma}$ can be derived and $\tilde{\sigma}$ is the unique maximizer of the CE functional.

The convenience of adopting a CE formulation is apparent from the fact that the solution is characterized by a unique stress field while the displacements are in general indeterminate.

The functionals introduced in the previous paragraph are nonsmooth and nondifferentiable because of the presence of the indicator functional of the admissible stress domain $\mathscr{K}_\sigma$. Since the solution of the problem is expected to lie on the boundary of $\mathscr{K}_\sigma$ (apart from trivial cases) it is necessary, for numerical computations, to regularize the indicator functional. It is first observed that the set $\mathscr{K}_\sigma$ can be expressed in the following equivalent ways:

$$\mathscr{K}_\sigma = \left\{\sigma \in \mathscr{D}' : \sigma n \cdot n \leqslant 0 \ \forall n\right\} \tag{41}$$

$$= \left\{\sigma \in \mathscr{D}' : \max\left[\mathrm{eig}(\sigma)\right] \leqslant 0\right\} \tag{42}$$

$$= \left\{\sigma \in \mathscr{D}' : \mathrm{tr}(\sigma) \leqslant 0,\ \frac{\mathrm{tr}(\sigma)^2 - \mathrm{tr}(\sigma^2)}{2} \geqslant 0,\ \det(\sigma) \leqslant 0\right\} \tag{43}$$

or also, in the plane stress case,

$$\mathscr{K}_\sigma = \left\{\sigma \in \mathscr{D}' : \mathrm{tr}(\sigma) \leqslant 0,\ \frac{\mathrm{tr}(\sigma)^2 - \mathrm{tr}(\sigma^2)}{2} \geqslant 0\right\} \tag{44}$$

i.e. the admissibility of the stress state can be enforced through the sign of the maximum principal stress $\sigma_{\mathrm{M}} = \max\left[\mathrm{eig}(\sigma)\right]$ or through the stress invariants. Although in principle Eqs. (41) (44) are totally equivalent, in practical applications they differ because of the convexity and differentiability properties of the functions involved. The convexity properties can easily be verified using the principal stresses $\sigma_1, \sigma_2, \sigma_3$. Results obtained are presented in Table 1.

The set $\mathscr{K}_\sigma$ is thus described by one or more inequalities of the kind $h(\sigma) \leqslant 0$. Three commonly used regularisations for the functional $\mathrm{ind}_{\mathscr{K}_\sigma}$ are

$$\mathrm{ind}_{\mathscr{K}_\sigma} = \lim_{\alpha \to +\infty} \tfrac{1}{2}\alpha \langle h(\sigma)\rangle^2, \tag{45}$$

$$\mathrm{ind}_{\mathscr{K}_\sigma} = \sup_{\lambda \geqslant 0} \lambda h(\sigma), \tag{46}$$

$$\mathrm{ind}_{\mathscr{K}_\sigma} = \sup_{\lambda \in \mathscr{R}} \left[\lambda h(\sigma)^+ + \tfrac{1}{2}\alpha\left(h(\sigma)^+\right)^2\right] \quad \forall \alpha > 0, \tag{47}$$

respectively, called penalty, Lagrangian and augmented Lagrangian regularisation. In (45) $\langle\ \rangle$ is the McCauley bracket ($\langle x\rangle = x$ if $x \geqslant 0$, $\langle x\rangle = 0$ otherwise) and in (47) the inequality constraint $h(\sigma) \leqslant 0$ is converted into an equality one. In fact, the following equivalences hold

$$h(\sigma) \leqslant 0 \text{ is equivalent to } h(\sigma)^+ = \max\left(h(\sigma), -\lambda/\alpha\right) = 0, \tag{48}$$

$$h(\sigma) \geqslant 0 \text{ is equivalent to } h(\sigma)^- = \min\left(h(\sigma), -\lambda/\alpha\right)$$

$$= -\max\left(-h(\sigma), \lambda/\alpha\right) = 0, \tag{49}$$

where provided $h(\sigma)$ is differentiable in its admissible subspace, the functions $h(\sigma)^+$ and $h(\sigma)^-$ are differentiable as well [18]. Equivalence (47) is proved below.

Table 1
Convexity of the constraint functionals and their squares

Convex	σ_{M}	tr (σ)		$\mathrm{tr}(\sigma)^2$		
Nonconvex	σ_{M}^2	$(\mathrm{tr}(\sigma)^2$	$\mathrm{tr}(\sigma^2))/2$	$\left[(\mathrm{tr}(\sigma)^2$	$\mathrm{tr}(\sigma^2))/2\right]^2$	$\det(\sigma)$	$\det(\sigma)^2$

For equivalence (47) to hold we must have

$$h(\sigma) > 0 \quad \Rightarrow \quad \sup_{\lambda \in \mathscr{R}} \left[\lambda h(\sigma)^+ + \tfrac{1}{2}\alpha \left(h(\sigma)^+ \right)^2 \right] = +\infty, \tag{50}$$

$$h(\sigma) \leqslant 0 \quad \Rightarrow \quad \sup_{\lambda \in \mathscr{R}} \left[\lambda h(\sigma)^+ + \tfrac{1}{2}\alpha \left(h(\sigma)^+ \right)^2 \right] = 0. \tag{51}$$

By definition

$$h^+(\sigma) = \begin{cases} h(\sigma) & \text{if } \lambda \geqslant -\alpha h(\sigma), \\ -\lambda/\alpha & \text{if } \lambda < -\alpha h(\sigma). \end{cases} \tag{52}$$

If $\lambda < -\alpha h(\sigma)$, by substitution into (47) we find

$$\sup_{\substack{\lambda \in \mathscr{R} \\ \lambda < -\alpha h(\sigma)}} \left[\lambda h(\sigma)^+ + \tfrac{1}{2}\alpha \left(h(\sigma)^+ \right)^2 \right] = \sup_{\substack{\lambda \in \mathscr{R} \\ \lambda < -\alpha h(\sigma)}} \left[-\tfrac{1}{2}\alpha h(\sigma)^2 \right] = 0. \tag{53}$$

If $\lambda \geqslant -\alpha h(\sigma)$, we find

$$\begin{aligned} \sup_{\substack{\lambda \in \mathscr{R} \\ \lambda \geqslant -\alpha h(\sigma)}} \left[\lambda h(\sigma)^+ + \tfrac{1}{2}\alpha \left(h(\sigma)^+ \right)^2 \right] &= \sup_{\substack{\lambda \in \mathscr{R} \\ \lambda \geqslant -\alpha h(\sigma)}} \left[\lambda h(\sigma) + \tfrac{1}{2}\alpha h(\sigma)^2 \right] \\ &= \begin{cases} -\tfrac{1}{2}\alpha h(\sigma)^2 & \text{if } h(\sigma) \leqslant 0, \\ +\infty & \text{if } h(\sigma) > 0. \end{cases} \end{aligned} \tag{54}$$

From (53) and (54) the thesis that immediately follows is

$$\sup_{\lambda \in \mathscr{R}} \left[\lambda h(\sigma)^+ + \tfrac{1}{2}\alpha \left(h(\sigma)^+ \right)^2 \right] = \begin{cases} 0 & \text{if } h(\sigma) \leqslant 0, \\ +\infty & \text{if } h(\sigma) > 0. \end{cases} \tag{55}$$

Penalty methods have been extensively used in unilateral and no-tension problems [19,10]. However, since the limit (45) cannot be computed exactly to avoid ill conditioning, it leads to a relaxation of the constraint condition. Lagrangian multiplier methods are less frequently adopted in no-tension problems in conjunction with displacement formulations. Augmented Lagrangian methods are well established in contact problems where they have proved to be very efficient and reliable [20,21] and their first application to no-tension problems was presented in Cuomo and Ventura [22,23]. They allow the admissibility constraint to be strictly enforced, at the same time avoiding the drawbacks of both the penalty and the Lagrangian multiplier approaches.

In the following subsections the augmented Lagrangian regularisations for the different constraints (42) (44) will be considered.

2.5.1. Regularisation in the stress invariants

Introducing the following notations

$$\begin{aligned} I_1 &= \operatorname{tr}(\sigma), \\ I_2 &= \frac{\operatorname{tr}(\sigma)^2 - \operatorname{tr}(\sigma^2)}{2}, \\ I_3 &= \det(\sigma), \end{aligned} \tag{56}$$

the augmented Lagrangian regularisation of expression (43) for the indicator functional is obtained

$$\operatorname{ind}_{\mathscr{K}_\sigma}(\sigma) = \sup_{\lambda_1, \lambda_2, \lambda_3 \in \mathscr{R}} \lambda_1 I_1^+ + \lambda_2 I_2^- + \lambda_3 I_3^+ + \tfrac{1}{2}\alpha \left[I_1^{+^2} + I_2^{-^2} + I_3^{+^2} \right] \tag{57}$$

or, in the plane stress case,

$$\operatorname{ind}_{\mathscr{K}_\sigma}(\sigma) = \sup_{\lambda_1, \lambda_2 \in \mathscr{R}} \lambda_1 I_1^+ + \lambda_2 I_2^- + \tfrac{1}{2}\alpha \left[I_1^{+^2} + I_2^{-^2} \right]^2. \tag{58}$$

In (57) and (58) a single penalty parameter α has been used for all the constraints for the sake of simplicity, but different penalty parameters for each constraint are sometimes convenient.

2.5.2. Regularisation in the maximum principal stress

Let σ_{M} be the maximum principal stress. The following regularisation is considered:

$$\mathrm{ind}_{\mathscr{K}_\sigma}(\sigma) = \sup_{\lambda \in \mathscr{R}} \left[\lambda \sigma_{\mathrm{M}}^{+} + \tfrac{1}{2}\alpha \left(\sigma_{\mathrm{M}}^{+}\right)^2 \right]. \tag{59}$$

In the plane stress case, assuming xy to be the stress plane, σ_{M} is given by the real quantity

$$\sigma_{\mathrm{M}} = \frac{\sigma_x + \sigma_y}{2} + \sqrt{\frac{\left(\sigma_x - \sigma_y\right)^2}{4} + \tau_{xy}^2}. \tag{60}$$

In the triaxial case algebraic expressions for the principal stresses can be obtained in a closed form. Let I_1, I_2, I_3 be the stress invariants defined in the previous paragraph and let us define the following quantities

$$a = 3I_2 - I_1^2, \tag{61}$$

$$b = 2I_1^3 - 9I_1 I_2 + 27I_3, \tag{62}$$

$$c = \sqrt[3]{b + \sqrt{b^2 + 4a}}. \tag{63}$$

The principal stresses are thus given by

$$\sigma_1 = \frac{I_1}{3} - \frac{a\sqrt[3]{2}}{c} + \frac{c}{\sqrt[3]{32}}, \tag{64}$$

$$\sigma_2 = \frac{I_1}{3} + \frac{a\left(1 + \mathrm{i}\sqrt{3}\right)}{c\sqrt[3]{32^2}} - \frac{c\left(1 - \mathrm{i}\sqrt{3}\right)}{\sqrt[3]{62}}, \tag{65}$$

$$\sigma_3 = \frac{I_1}{3} + \frac{a\left(1 - \mathrm{i}\sqrt{3}\right)}{c\sqrt[3]{32^2}} - \frac{c\left(1 + \mathrm{i}\sqrt{3}\right)}{\sqrt[3]{62}} \tag{66}$$

and $\sigma_{\mathrm{M}} = \max(\sigma_1, \sigma_2, \sigma_3)$. In the preceding equations it should be noted that, even if the imaginary quantity i appears, the principal stresses are of course real numbers (being the eigenvalues of a symmetric real tensor) and the quantity c turns out to be a complex number (otherwise $\mathrm{Im}(c) = 0 \Rightarrow \sigma_2 = \sigma_3$).

2.6. Variational principles differentiable form

As pointed out in the preceding sections, the generalized Hellinger Reissner functional (35) and the CE functional (40) are nondifferentiable because of the presence of the indicator function of the admissible stress domain. Equivalent smooth and differentiable functional and variational principles can easily be obtained by substituting the augmented Lagrangian regularisations of $\mathrm{ind}_{\mathscr{K}_\sigma}$.

If principal stress regularisation is chosen, by introducing (59) into the CE functional (40) and changing the sign of all the terms, a functional $\Pi_{\mathrm{C}}^{\mathrm{al}}(\sigma, \lambda)$ is obtained and the following saddle point characterizes the solution of the equilibrium problem for a no-tension solid

$$\sup_{\lambda \in \mathscr{R}} \min_{\sigma \in \mathscr{K}_{\mathrm{e}}} \Pi_{\mathrm{C}}^{\mathrm{al}}(\sigma, \lambda). \tag{67}$$

In (67) both the function σ_{M} and σ_{M}^2 appear, Eq. (59). While σ_{M} is a convex function and it can easily be verified that its Hessian $\nabla^2 \sigma_{\mathrm{M}}$ is positive semidefinite in the whole stress space, it should be noted, as pointed out in Table 1, that its square is positive semidefinite only when $\sigma_{\mathrm{M}} \geqslant 0$ (i.e. whenever the constraint is active), as $\nabla^2(\sigma_{\mathrm{M}}^2) = 2\sigma_{\mathrm{M}} \nabla^2 \sigma_{\mathrm{M}}$. This observation must to be taken into account in the numerical implementation of solution algorithms, as the square of σ_{M} is the only nonconvex term in the stress variables.

In the same way, if stress invariant regularisation is chosen, by introducing Eqs. (57) into the CE functional (40) and changing the sign of all the terms, a functional $\Pi_{\mathrm{C}}^{\mathrm{al}}(\sigma, \lambda_1, \lambda_2, \lambda_3)$ is obtained and again the following saddle point characterizes the solution of the equilibrium problem

$$\sup_{\lambda_1,\lambda_2,\lambda_3 \in \mathscr{R}} \min_{\sigma \in \mathscr{K}_{\mathrm{e}}} \Pi_{\mathrm{C}}^{\mathrm{al}}(\sigma, \lambda_1, \lambda_2, \lambda_3) \tag{68}$$

or, in the plane stress case, by introducing (58),

$$\sup_{\lambda_1,\lambda_2 \in \mathscr{R}} \min_{\sigma \in \mathscr{K}_{\mathrm{e}}} \Pi_{\mathrm{C}}^{\mathrm{al}}(\sigma, \lambda_1, \lambda_2). \tag{69}$$

Although the stress invariants, as compared to the principal stresses, have a simpler mathematical form, regularisations (57) and (58) involve different convexity properties of the constraints (see Table 1).

2.7. Stress space reduction

The CE functionals and the saddle point problems introduced in the previous section are defined on the space of equilibrated stresses, $\sigma \in \mathscr{K}_{\mathrm{e}}$. However, the definition of the set $\mathscr{K}_{\mathrm{e}}$ is too strong and can be relaxed. In fact, in the definition of the CE functional the equilibrium equations only need to be satisfied in a weak form and a considerably larger stress space can be considered, i.e. $\mathscr{K}_{\mathrm{e}}$ can be more conveniently redefined as

$$\mathscr{K}_{\mathrm{e}} = \left\{ \sigma \in \mathscr{D}' : \left\langle C'\sigma - b, v \right\rangle_0 + \langle P\sigma - q_{\mathrm{d}} - \mu q_{\mathrm{l}}, v \rangle_{\partial \mathscr{B}_q} = 0 \ \forall u \in \mathscr{V} \right\}. \tag{70}$$

Introducing the space $\mathscr{K}_{\mathrm{e}}^0 = \ker(C')$ of the self-equilibrated stresses and the complementary space K_{e}^1 of the stresses in equilibrium with the external loads

$$\mathscr{K}_{\mathrm{e}}^0 = \left\{ \sigma \in \mathscr{D}' : \left\langle C'\sigma, v \right\rangle_0 + \langle P\sigma, v \rangle_{\partial \mathscr{B}_q} = 0 \ \forall u \in \mathscr{V} \right\}, \tag{71}$$

$$\mathscr{K}_{\mathrm{e}}^1 = \left\{ \sigma \in \mathscr{D}' : \left\langle C'\sigma - b, v \right\rangle_0 + \langle P\sigma - q_{\mathrm{d}} - \mu q_{\mathrm{l}}, v \rangle_{\partial \mathscr{B}_q} = 0 \ \forall u \in \mathscr{V} \right\} \tag{72}$$

the space $\mathscr{K}_{\mathrm{e}} = \mathscr{K}_{\mathrm{e}}^0 \oplus \mathscr{K}_{\mathrm{e}}^1$ can be generated through the elements of $\mathscr{K}_{\mathrm{e}}^0$ and an arbitrary fixed element belonging to $\mathscr{K}_{\mathrm{e}}^1$

$$\mathscr{K}_{\mathrm{e}} = \left\{ \sigma = \sigma_0 + \sigma_1 : \sigma_0 \in \mathscr{K}_{\mathrm{e}}^0, \ \text{ given } \sigma_1 \in \mathscr{K}_{\mathrm{e}}^1 \right\}. \tag{73}$$

In the finite element implementation of the problem the decomposition (73) of the set $\mathscr{K}_{\mathrm{e}}$ is especially useful, as it leads to a significant reduction in the number of discrete stress variables.

2.8. Computation of the inelastic deformation field

Inelastic deformations can be readily determined by introducing augmented Lagrangian regularisations of the indicator functional in the constitutive equation (16). As the regularisations are differentiable the explicit expressions of the inelastic deformations are obtained from (16) taking their gradients w.r.t. the stress components. The constraint functional appearing in the regularisation of $\mathrm{ind}_{\mathscr{K}_\sigma}$ thus plays a role similar to that of the yield functional in the classical theory of associated plasticity, except that, in the present case, the total value of the inelastic deformation appears instead of its rate. This is a direct consequence of the fact that no-tension materials exhibit reversible behaviour. The explicit evaluation of (16) is reported distinguishing between principal stress and invariant regularisations.

2.8.1. Regularisation in the maximum principal stress

From (16) and the augmented Lagrangian regularisation (59) the inelastic deformation takes the form

$$\varepsilon^{\mathrm{a}} = \left(\lambda + \alpha \sigma_{\mathrm{M}}^{+}\right) \nabla \sigma_{\mathrm{M}}^{+}. \tag{74}$$

When the solution of the problem is obtained, $\sigma_M^+ = 0$ and
- if the constraint is active then $\sigma_M = 0$, $\lambda > 0$,
- if the constraint is not active then $\sigma_M < 0$, $\lambda = 0$

so expression (74) can be simplified into

$$\varepsilon^a = \lambda \nabla \sigma_M, \tag{75}$$

which can be written in tensor form

$$\varepsilon^a = \lambda \begin{bmatrix} \frac{\partial \sigma_M}{\partial \sigma_x} & \frac{1}{2}\frac{\partial \sigma_M}{\partial \tau_{xy}} & \frac{1}{2}\frac{\partial \sigma_M}{\partial \tau_{xz}} \\ \frac{1}{2}\frac{\partial \sigma_M}{\partial \tau_{xy}} & \frac{\partial \sigma_M}{\partial \sigma_y} & \frac{1}{2}\frac{\partial \sigma_M}{\partial \tau_{yz}} \\ \frac{1}{2}\frac{\partial \sigma_M}{\partial \tau_{xz}} & \frac{1}{2}\frac{\partial \sigma_M}{\partial \tau_{yz}} & \frac{\partial \sigma_M}{\partial \sigma_z} \end{bmatrix} = \lambda W(\sigma). \tag{76}$$

It can be verified that the eigenvalues of $W(\sigma)$ are $(0, 0, 1)$ and its eigenvectors coincide with the principal stress directions. This means that the Lagrangian multiplier λ has the physical meaning of the inelastic deformation dual to σ_M, i.e. $\lambda \equiv \varepsilon_M^a$.

2.8.2. Regularisation in the stress invariants

Using (57) the following expression for the inelastic deformation is obtained

$$\varepsilon^a = \left(\lambda_1 + \alpha I_1^+\right)\nabla I_1^+ + \left(\lambda_2 + \alpha I_2^-\right)\nabla I_2^- + \left(\lambda_3 + \alpha I_3^+\right)\nabla I_3^+ \tag{77}$$

and, in the plane stress case,

$$\varepsilon^a = \left(\lambda_1 + \alpha I_1^+\right)\nabla I_1^+ + \left(\lambda_2 + \alpha I_2^-\right)\nabla I_2^-. \tag{78}$$

When the solution is obtained, $\sigma_1 \leqslant 0$, $\sigma_2 \leqslant 0$, $\sigma_3 \leqslant 0$. Except for the trivial case when $\sigma_1 = \sigma_2 = \sigma_3 = 0$ and the deformation field is indeterminate $I_1 = \mathrm{tr}(\sigma) < 0$ always holds and it is therefore an inactive constraint. Thus the following cases can occur:
- $\sigma_1 < 0$, $\sigma_2 = \sigma_3 = 0$: both I_2 and I_3 are active constraints, but $\nabla I_3 \equiv 0$;
- $\sigma_1 < 0$, $\sigma_2 < 0, \sigma_3 = 0$: the only active constraint is I_3;
- $\sigma_1 < 0$, $\sigma_2 < 0, \sigma_3 < 0$: no constraints are active.

Summarising in bidimensional analysis we have

$$\varepsilon^a = \lambda_2 \nabla I_2 \tag{79}$$

and in three-dimensional analysis, if the solution gives a plane stress state,

$$\varepsilon^a = \lambda_3 \nabla I_3 \tag{80}$$

while, if the solution gives a uniaxial stress state,

$$\varepsilon^a = \lambda_2 \nabla I_2. \tag{81}$$

3. Finite element formulation

3.1. Discretisation of the field variables

The numerical solution of the saddle point problem arising from the regularized forms of the CE functionals (67) (69) can be obtained in the framework of the finite element method through the introduction of suitable interpolation functions for all the fields appearing in the continuous formulation.

Indicating with **G** the matrix of element shape functions the following stress interpolation is assumed:

$$\sigma = \mathbf{G}_\sigma \mathbf{s} \tag{82}$$

The displacement field u is interpolated for the sake of convenience by separating the displacements in $\mathrm{Int}(\mathscr{B}) \cup \partial\mathscr{B}_q$ and those on its frontier $\partial\mathscr{B}_u$

$$u = \begin{bmatrix} v \\ \overline{u} \end{bmatrix} = \mathbf{G}_{ut}\mathbf{u}_t = \begin{bmatrix} \mathbf{G}_u & \mathbf{0} \\ \mathbf{0} & \mathbf{G}_{\overline{u}} \end{bmatrix} \quad \begin{bmatrix} \mathbf{u} \\ \overline{\mathbf{u}} \end{bmatrix}. \tag{83}$$

3.2. Discretisation of equilibrium and compatibility equations

The Gauss formula

$$\langle \sigma, Cv \rangle_{\mathscr{D}} = -\langle C'\sigma, v \rangle_0 + \langle \mathrm{P}\sigma, w \rangle_{\partial\mathscr{B}} \tag{84}$$

does not hold in the F.E. framework as the derivatives of the shape functions are in general discontinuous across the interelement boundaries. Eq. (84) is therefore valid at the element level but not on the whole mesh. In order to avoid the undesirable boundary terms appearing on the RHS of (84) the equilibrium equations are obtained directly from the discretised form of the Hellinger Reissner functional (35)

$$\begin{aligned} \Pi_{\mathrm{R}}^{\mathrm{d}}(\mathbf{s}, \mathbf{u}_t) = &-\frac{1}{2}\int_{\mathscr{B}} E^{-1}\mathbf{G}_\sigma\mathbf{s} \cdot \mathbf{G}_\sigma\mathbf{s}\,\mathrm{d}B - \int_{\mathscr{B}} \mathrm{ind}_{\mathscr{K}_\sigma}\,\mathrm{d}B + \int_{\mathscr{B}} \mathbf{G}_\sigma\mathbf{s} \cdot C\mathbf{G}_u\mathbf{u}\,\mathrm{d}B + \int_{\mathscr{B}} \mathbf{G}_\sigma\mathbf{s} \cdot C\mathbf{G}_{\overline{u}}\overline{\mathbf{u}}\,\mathrm{d}B \\ &- \int_{\mathscr{B}} b \cdot \mathbf{G}_u\mathbf{u}\,\mathrm{d}B - \int_{\partial\mathscr{B}_q} (q_{\mathrm{d}} + \mu q_{\mathrm{l}}) \cdot \mathbf{G}_u\mathbf{u}\,\mathrm{d}S - \int_{\partial\mathscr{B}_u} \mathrm{ind}_{\mathscr{W}}\,\mathrm{d}S, \end{aligned} \tag{85}$$

where $\mathscr{W} = \{u \in \mathscr{U} : u = \bar{u} \text{ on } \partial B_u\}$ and the last integral enforces the boundary conditions on the discretised displacements in a variational form. The nodal boundary displacements $\overline{\mathbf{u}}$ also appear in the volume integral as they determine the displacements of the region of $\mathrm{Int}(\mathscr{B})$ covered by the elements adjacent to the boundary. The discrete form of the term $\int_{\mathscr{B}} \mathrm{ind}_{\mathscr{K}_\sigma}\,\mathrm{d}B$ will be discussed in the next subsection.

Denoting with $\mathbf{F} = \int_{\mathscr{B}} \mathbf{G}_\sigma^{\mathrm{T}} E^{-1}\mathbf{G}_\sigma\,\mathrm{d}B$ the flexibility matrix and letting $\mathbf{b} = \int_{\mathscr{B}} \mathbf{G}_u^{\mathrm{T}} b\,\mathrm{d}B$, $\mathbf{q}_{\mathrm{d}} = \int_{\partial\mathscr{B}_q} \mathbf{G}_u^{\mathrm{T}} q_{\mathrm{d}}\,\mathrm{d}S$, $\mathbf{q}_{\mathrm{l}} = \int_{\partial\mathscr{B}_q} \mathbf{G}_u^{\mathrm{T}} q_{\mathrm{l}}\,\mathrm{d}S$, $\mathbf{C} = \int_{\mathscr{B}} (C\mathbf{G}_u)^{\mathrm{T}}\mathbf{G}_\sigma\,\mathrm{d}B$, $\mathbf{H} = \int_{\mathscr{B}} (C\mathbf{G}_{\bar{u}})^{\mathrm{T}}\mathbf{G}_\sigma\,\mathrm{d}B$, using the Lagrangian regularisation for the boundary constraint, expression (85) becomes

$$\begin{aligned} \Pi_{\mathrm{R}}^{\mathrm{d}}(\mathbf{s}, \mathbf{u}_t) = &-\tfrac{1}{2}\mathbf{F}\mathbf{s} \cdot \mathbf{s} - \mathbf{b} \cdot \mathbf{u} - (\mathbf{q}_{\mathrm{d}} + \mu\mathbf{q}_{\mathrm{l}}) \cdot \mathbf{u} + \mathbf{C}\mathbf{u} \cdot \mathbf{s} + \mathbf{H}\overline{\mathbf{u}} \cdot \mathbf{s} \\ &- \mathbf{r} \cdot \overline{\mathbf{u}} + \int_{\partial\mathscr{B}_u} \rho \cdot \bar{u}\,\mathrm{d}S - \int_{\mathscr{B}} \mathrm{ind}_{\mathscr{K}_\sigma}\,\mathrm{d}B \end{aligned} \tag{86}$$

with $\mathbf{r} = \int_{\partial\mathscr{B}_u} \mathbf{G}_{\bar{u}}^{\mathrm{T}} \rho\,\mathrm{d}S$ and $\mathbf{r} \cdot \overline{\mathbf{u}} = \int_{\partial\mathscr{B}_u} \rho \cdot \bar{u}\,\mathrm{d}S$.

By equating to zero the variations of $\Pi_{\mathrm{R}}^{\mathrm{d}}$ w.r.t. the unknown displacements $\mathbf{u}$ and the prescribed ones $\overline{\mathbf{u}}$, the discrete equilibrium equations are determined:

$$\mathbf{C}^{\mathrm{T}}\mathbf{s} = \mathbf{b} + \mathbf{q}_{\mathrm{d}} + \mu\mathbf{q}_{\mathrm{l}}, \tag{87}$$

$$\mathbf{H}^{\mathrm{T}}\mathbf{s} = \mathbf{r}. \tag{88}$$

Using (87) and (88) in (86) and performing a sign reversal the following CE functional is obtained:

$$\Pi_{\mathrm{C}}^{\mathrm{d}}(\mathbf{s}) = \frac{1}{2}\mathbf{F}\mathbf{s} \cdot \mathbf{s} - \mathbf{r} \cdot \overline{\mathbf{u}} + \int_{\mathscr{B}} \mathrm{ind}_{\mathscr{K}_\sigma}\,\mathrm{d}B, \quad \mathbf{s} \in \mathscr{Y}_{\mathrm{e}}, \tag{89}$$

$$\mathscr{Y}_{\mathrm{e}} = \{\mathbf{s} : \mathbf{C}^{\mathrm{T}}\mathbf{s} = \mathbf{b} + \mathbf{q}_{\mathrm{d}} + \mu\mathbf{q}_{\mathrm{l}}\}, \tag{90}$$

$\mathscr{Y}_{\mathrm{e}}$ being the set of nodal equilibrated stresses, i.e. the discretised counterpart of $\mathscr{K}_{\mathrm{e}}$. In general $\mathscr{K}_{\mathrm{e}} \neq \mathscr{Y}_{\mathrm{e}}$ and, as observed in the continuum formulation, the set $\mathscr{Y}_{\mathrm{e}}$ can be split into the set $\mathscr{Y}_{\mathrm{e}}^0$ of self-equilibrated nodal stresses and the set $\mathscr{Y}_{\mathrm{e}}^1$ of nodal stresses in equilibrium with the prescribed body and surface loads.

$$\mathscr{Y}_{\mathrm{e}}^0 = \{\mathbf{s} : \mathbf{C}^{\mathrm{T}}\mathbf{s} = \mathbf{0}\}, \tag{91}$$

$$\mathscr{Y}_{\mathrm{e}}^1 = \{\mathbf{s} : \mathbf{C}^{\mathrm{T}}\mathbf{s} = \mathbf{b} + \mathbf{q}_{\mathrm{d}} + \mu\mathbf{q}_{\mathrm{l}}\}. \tag{92}$$

The affine linear manifold $\mathscr{Y}_e$ is generated by the elements of $\mathscr{Y}_e^0$ and an arbitrary fixed element belonging to $\mathscr{Y}_e^1$

$$\mathscr{Y}_e = \{\mathbf{s} = \mathbf{s}_0 + \mathbf{s}_1 : \mathbf{s}_0 \in \mathscr{Y}_e^0, \text{ given } \mathbf{s}_1 \in \mathscr{Y}_e^1\}. \tag{93}$$

While in the continuum problem the subsets $\mathscr{K}_e^0$ and $\mathscr{K}_e^1$ cannot be given an explicit representation ($\mathscr{K}_e$ not being finite dimensional), the decomposition (93) can be expressed in a closed form. In fact, if n is the number of nodes, n_d the number of space dimensions and v is the number of constrained degrees of freedom (fixed displacement components) then the above-defined matrices and vectors have the following dimensions

Symbol	Description	Dimensions (rows by columns)
$\mathbf{s}$	nodal stresses	$n_s = n,\ 3n,\ 6n$ for $n_d = 1, 2, 3$
$\bar{\mathbf{u}}$	prescribed displacements on $\partial\mathscr{B}_u$	v
$\mathbf{b}$, $\mathbf{q}_d$, $\mathbf{q}_l$	equivalent nodal loads	$nn_d - v$
$\mathbf{C}^T$	equilibrium matrix	$nn_d - v \times n_s$
$\mathbf{H}^T$	constraint reaction operator	$v \times n_s$
$\mathbf{F}$	flexibility matrix	$n_s \times n_s$
$\mathbf{r}$	constraint reactions	v

In the hypothesis that no rigid body motion is allowed, the equilibrium matrix $\mathbf{C}^T$ has a rank of $nn_d - v$. In fact $nn_d - v \leqslant n_s$ and if $\operatorname{rank}(\mathbf{C}^T) < nn_d - v$ then the image of $\mathbf{C}^T$ would not cover the entire space $\mathbb{R}^{nn_d - v}$ and $\infty^{(nn_d - v) - \operatorname{rank}(\mathbf{C}^T)}$ equivalent nodal load vectors could be found such that no equilibrating nodal stress vector $\mathbf{s}$ exists. It follows that there is at least one suitable ordering of the components of $\mathbf{s}$ such that

$$\mathbf{C}^T\mathbf{s} = \begin{bmatrix}\mathbf{C}_0^T & \mathbf{C}_1^T\end{bmatrix}\begin{bmatrix}\mathbf{s}_0 \\ \mathbf{s}_1\end{bmatrix} = \mathbf{C}_0^T\mathbf{s}_0 + \mathbf{C}_1^T\mathbf{s}_1, \tag{94}$$

where the matrix $\mathbf{C}_1^T$ is $nn_d - v \times nn_d - v$ and has full rank (i.e. it is nonsingular) and $\mathbf{s}_0$, $\mathbf{s}_1$ are vectors of order $nn_d - v$ and $n_s - nn_d + v$, respectively. The equilibrium equations (87) are condensed as follows:

$$\mathbf{C}_0^T\mathbf{s}_0 + \mathbf{C}_1^T\mathbf{s}_1 = \mathbf{b} + \mathbf{q}_d + \mu\mathbf{q}_l, \tag{95}$$

$$\mathbf{s}_1 = \mathbf{C}_1^{-T}\big(-\mathbf{C}_0^T\mathbf{s}_0 + \mathbf{b} + \mathbf{q}_d + \mu\mathbf{q}_l\big), \tag{96}$$

$$\mathbf{s} = \begin{bmatrix}\mathbf{s}_0 \\ \mathbf{s}_1\end{bmatrix} = \begin{bmatrix}\mathbf{I} \\ -\mathbf{C}_1^{-T}\mathbf{C}_0^T\end{bmatrix}\mathbf{s}_0 + \begin{bmatrix}\mathbf{0} \\ \mathbf{C}_1^{-T}(\mathbf{b} + \mathbf{q}_d + \mu\mathbf{q}_l)\end{bmatrix}. \tag{97}$$

Introducing the positions

$$\mathbf{R} = \begin{bmatrix}\mathbf{I} \\ -\mathbf{C}_1^{-T}\mathbf{C}_0^T\end{bmatrix};\quad \mathbf{t}_d = \begin{bmatrix}\mathbf{0} \\ \mathbf{C}_1^{-T}(\mathbf{b} + \mathbf{q}_d)\end{bmatrix};\quad \mathbf{t}_l = \begin{bmatrix}\mathbf{0} \\ \mathbf{C}_1^{-T}\mathbf{q}_l\end{bmatrix}, \tag{98}$$

Eq. (97) is rewritten in compact form as

$$\mathbf{s} = \mathbf{R}\mathbf{s}_0 + \mathbf{t}_d + \mu\mathbf{t}_l. \tag{99}$$

The form of (97) can be conveniently determined in computations through a suitable Gaussian reduction which is also numerically very stable. In this way a considerable reduction in the number of unknowns is obtained.

The column reordering performed on $\mathbf{C}^T$ is reproduced on the flexibility matrix $\mathbf{F}$ and on the reaction operator $\mathbf{H}^T$. The discretised CE functional (89) can be given the form

$$\Pi_C^d(\mathbf{s}_0) = \frac{1}{2}\begin{bmatrix}\mathbf{F}_{00} & \mathbf{F}_{10} \\ \mathbf{F}_{01} & \mathbf{F}_{11}\end{bmatrix}\begin{bmatrix}\mathbf{s}_0 \\ \mathbf{s}_1(\mathbf{s}_0)\end{bmatrix}\cdot\begin{bmatrix}\mathbf{s}_0 \\ \mathbf{s}_1(\mathbf{s}_0)\end{bmatrix} - \begin{bmatrix}\mathbf{H}_0^T & \mathbf{H}_1^T\end{bmatrix}\begin{bmatrix}\mathbf{s}_0 \\ \mathbf{s}_1(\mathbf{s}_0)\end{bmatrix}\cdot\bar{\mathbf{u}} + \int_{\mathscr{B}} \operatorname{ind}_{\mathscr{K}_\sigma}\, dB. \tag{100}$$

By introducing (99), calculating the products and dropping the inessential constant terms, the following final form is obtained

$$\Pi_{\mathrm{C}}^{\mathrm{d}}(\mathbf{s}_0) = \frac{1}{2}\mathbf{R}^{\mathrm{T}}\mathbf{F}\mathbf{R}\,\mathbf{s}_0 \cdot \mathbf{s}_0 + \mathbf{R}^{\mathrm{T}}[\mathbf{F}(\mathbf{t}_{\mathrm{d}} + \mu\mathbf{t}_{\mathrm{l}}) - \mathbf{H}\bar{\mathbf{u}}] \cdot \mathbf{s}_0 + \int_{\mathscr{B}} \mathrm{ind}_{\mathscr{K}_\sigma}\,\mathrm{d}B. \tag{101}$$

The functional (101) just obtained is made up of a quadratic and a linear term in the self-equilibrated nodal stresses $\mathbf{s}_0$ and the nonlinear, nondifferentiable and l.s.c. term $\int_{\mathscr{B}} \mathrm{ind}_{\mathscr{K}_\sigma}\,\mathrm{d}B$.

3.3. Discrete form of the indicator functional

As pointed out in the previous section, the indicator functional $\mathrm{ind}_{\mathscr{K}_\sigma}$ is replaced by the augmented Lagrangian forms (57) (59). To achieve a uniform and clearer notation let

$$\mathrm{ind}_{\mathscr{K}_\sigma} = \sup_{\Lambda}\left(Q \cdot \Lambda + \tfrac{1}{2}\alpha Q \cdot Q\right), \tag{102}$$

where the meaning of the vectors Q (constraint functions) and Λ (Lagrangian multipliers) varies as shown in Table 2.

The integral of (102) is evaluated by adopting an appropriate number of Dirac delta functions for the multipliers, so that a collocation method is obtained. This approach leads to enforcement of the constraint at a discrete number of points, usually denominated as control points.

The discretised regularisation is therefore

$$\int_{\mathscr{B}} \mathrm{ind}_{\mathscr{K}_\sigma}\,\mathrm{d}B = \sup_{\Lambda}\left(\mathbf{Q} \cdot \Lambda + \tfrac{1}{2}\alpha\mathbf{Q} \cdot \mathbf{Q}\right), \tag{103}$$

where $\mathbf{Q}^{\mathrm{T}}(\mathbf{s}_0) = [Q_1^{\mathrm{T}}, Q_2^{\mathrm{T}}, \ldots, Q_{n_{\mathrm{cp}}}^{\mathrm{T}}]$ is the vector of the constraint functions evaluated at the n_{cp} control points and $\Lambda = [\Lambda_1^{\mathrm{T}}, \Lambda_2^{\mathrm{T}}, \ldots, \Lambda_{n_{\mathrm{cp}}}^{\mathrm{T}}]$ is the vector of the corresponding discrete Lagrangian multipliers. The vectors $\mathbf{Q}$ and Λ have dimensions equal to $n_{\mathrm{cp}}\dim(\Lambda)$, $\dim(\Lambda)$ being the dimension of the Λ vector.

Note that in Eq. (103) the Jacobian and the Gauss weights do not appear. More detailed comments on this point will be found in a forthcoming paper.

3.4. Discrete form of the variational principle

By introducing the approximation (103) the nonlinear augmented Lagrangian form of the complementary functional (101) is obtained:

$$\Pi_{\mathrm{C}}^{\mathrm{al}}(\mathbf{s}_0, \Lambda) = \tfrac{1}{2}\mathbf{R}^{\mathrm{T}}\mathbf{F}\mathbf{R}\,\mathbf{s}_0 \cdot \mathbf{s}_0 + \mathbf{R}^{\mathrm{T}}[\mathbf{F}(\mathbf{t}_{\mathrm{d}} + \mu\mathbf{t}_{\mathrm{l}}) - \mathbf{H}\bar{\mathbf{u}}] \cdot \mathbf{s}_0 + \mathbf{Q} \cdot \Lambda + \tfrac{1}{2}\alpha\mathbf{Q} \cdot \mathbf{Q}. \tag{104}$$

The solution of the discretised problem, provided it exists, is given by the saddle point

$$\min_{\mathbf{s}_0}\sup_{\Lambda}\Pi_{\mathrm{C}}^{\mathrm{al}}(\mathbf{s}_0, \Lambda). \tag{105}$$

The functional $\Pi_{\mathrm{C}}^{\mathrm{al}}(\mathbf{s}_0, \Lambda)$ is linear on the Lagrangian multipliers Λ but is nonlinear and in general nonconvex on the self-equilibrated stresses $\mathbf{s}_0$ as is evident from Table 1. However, as the admissible domain $\mathscr{K}_\sigma$ is convex, in practical applications properly chosen algorithms for the computation of the saddle point (105) can preserve the local convexity of $\Pi_{\mathrm{C}}^{\mathrm{al}}(\mathbf{s}_0, \Lambda)$ during iterations.

Table 2
Meaning of Q and Λ vectors

Regularisation	Q	Λ
Maximum principal stress	$Q^{\mathrm{T}}\ [\sigma_n^+]$	$\Lambda^{\mathrm{T}}\ [\lambda]$
Invariants (plane stress case)	$Q^{\mathrm{T}}\ [I_1^+,\ I_2\ ]$	$\Lambda^{\mathrm{T}}\ [\lambda_1,\ \lambda_2]$
Invariants (triaxial case)	$Q^{\mathrm{T}}\ [I_1^+,\ I_2\ ,\ I_3^+]$	$\Lambda^{\mathrm{T}}\ [\lambda_1,\ \lambda_2,\ \lambda_3]$

3.5. Determination of the nodal displacement field

Consistent nodal deformation definitions are obtained from the virtual work equality

$$\int_B (\varepsilon^e + \varepsilon^a) * \sigma \, dB = (\mathbf{e}^e + \mathbf{e}^a) \cdot \mathbf{s} \tag{106}$$

after introducing the F.E. interpolations and the constitutive equations for elastic and inelastic deformations (24) and (16)

$$\int_B \mathbf{G}_\sigma^T E^{-1} \mathbf{G}_\sigma \mathbf{s} \, dB \cdot \mathbf{s} + \int_B \mathbf{G}_\sigma^T \partial \mathrm{ind}_{\mathscr{K}_\sigma} \, dB \cdot \mathbf{s} = (\mathbf{e}^e + \mathbf{e}^a) \cdot \mathbf{s}. \tag{107}$$

The first term on the LHS of (107) yields the flexibility matrix $\mathbf{F}$. The second term is evaluated using (103) and the linearity of the subdifferential as follows

$$\begin{aligned} \int_B \mathbf{G}_\sigma^T \partial \mathrm{ind}_{\mathscr{K}_\sigma} \, dB &= \int_B \nabla_{\mathbf{s}}^T \sigma \partial \mathrm{ind}_{\mathscr{K}_\sigma}[\sigma(\mathbf{s})] \, dB = \int_B \partial_{\mathbf{s}} \mathrm{ind}_{\mathscr{K}_\sigma}[\sigma(\mathbf{s})] \, dB = \partial_{\mathbf{s}} \int_B \mathrm{ind}_{\mathscr{K}_\sigma}[\sigma(\mathbf{s})] \, dB \\ &= \partial_{\mathbf{s}}(\mathbf{Q} \cdot \Lambda + \tfrac{1}{2}\alpha \mathbf{Q} \cdot \mathbf{Q}) = \Lambda \cdot \mathbf{G}_\sigma^T \nabla_\sigma \mathbf{Q} + \alpha \mathbf{Q} \cdot \mathbf{G}_\sigma^T \nabla_\sigma \mathbf{Q} = (\Lambda + \alpha \mathbf{Q}) \cdot \mathbf{G}_\sigma^T \nabla_\sigma \mathbf{Q}. \end{aligned} \tag{108}$$

Inserting (108) into (107) the following definitions of elastic, inelastic and total nodal deformations are obtained:

$$\mathbf{e}^e = \mathbf{F}\mathbf{s}, \tag{109}$$

$$\mathbf{e}^a = (\Lambda + \alpha \mathbf{Q}) \cdot \mathbf{G}_\sigma^T \nabla_\sigma \mathbf{Q}, \tag{110}$$

$$\mathbf{e} = \mathbf{e}^e + \mathbf{e}^a. \tag{111}$$

Note that the quantities appearing in the definition of the inelastic deformations $\mathbf{e}^a$, referring to the nodes of the mesh, are evaluated at the control points.

The displacements can be evaluated from the compatibility equations obtained by equating to zero the variation w.r.t. $\mathbf{s}$ of the discretised Reissner functional (86). Using regularisation (103) we obtain

$$\mathbf{C}\mathbf{u} = \mathbf{F}\mathbf{s} + \nabla_{\mathbf{s}} \sigma \nabla_\sigma (\mathbf{Q} \cdot \Lambda + \tfrac{1}{2}\alpha \mathbf{Q} \cdot \mathbf{Q}) - \mathbf{H}\bar{\mathbf{u}} = \mathbf{e} - \mathbf{H}\bar{\mathbf{u}} \tag{112}$$

that is easily interpreted in the light of definitions (109) (111). By introducing partition (94) for $\mathbf{C}$ and the corresponding ones for $\mathbf{e}$ and $\mathbf{H}$ the following two matrix equations are obtained:

$$\begin{bmatrix} \mathbf{C}_0 \\ \mathbf{C}_1 \end{bmatrix} \mathbf{u} = \begin{bmatrix} \mathbf{e}_0 \\ \mathbf{e}_1 \end{bmatrix} - \begin{bmatrix} \mathbf{H}_0 \\ \mathbf{H}_1 \end{bmatrix} \bar{\mathbf{u}}. \tag{113}$$

$\mathbf{C}_1$ being nonsingular the second row of Eq. (113) can be inverted to yield the displacement field at the solution as a function of the stress state through $\mathbf{e}_1$

$$\mathbf{u} = \mathbf{C}_1^{-1} \mathbf{e}_1 - \mathbf{C}_1^{-1} \mathbf{H}_1 \bar{\mathbf{u}}. \tag{114}$$

The first row of Eq. (113) is identically satisfied since it is the Euler Lagrange equation obtained from the variation of (104) w.r.t. $\mathbf{s}_0$. In fact, by substituting (114) into the first row of (113) one has

$$\mathbf{e}_0 - \mathbf{C}_0 \mathbf{C}_1^{-1} \mathbf{e}_1 + \mathbf{C}_0 \mathbf{C}_1^{-1} \mathbf{H}_1 \bar{\mathbf{u}} - H_0 \bar{\mathbf{u}} = \mathbf{0}. \tag{115}$$

This equation, observing that $\mathbf{R}^T = \left[\mathbf{I} - \mathbf{C}_0 \mathbf{C}_1^{-1}\right]$, can be rewritten as

$$\mathbf{R}^T [\mathbf{e} - \mathbf{H}\bar{\mathbf{u}}] = \mathbf{0}. \tag{116}$$

On the other hand, equating to zero the variation of (104) w.r.t. $\mathbf{s}_0$ and using (99), it follows that

$$\mathbf{R}^{\mathrm{T}}\mathbf{F}\mathbf{R}\,\mathbf{s}_0 + \mathbf{R}^{\mathrm{T}}[\mathbf{F}(\mathbf{t}_{\mathrm{d}} + \mu\mathbf{t}_{\mathrm{l}}) - \mathbf{H}\bar{\mathbf{u}}] + \nabla_{\mathbf{s}_0}\mathbf{s}\,\nabla_{\mathbf{s}}\sigma\nabla_{\sigma}(\mathbf{Q}\cdot\Lambda + \tfrac{1}{2}\alpha\mathbf{Q}\cdot\mathbf{Q}) = \mathbf{0},$$

$$\mathbf{R}^{\mathrm{T}}\mathbf{F}\mathbf{R}\,\mathbf{s}_0 + \mathbf{R}^{\mathrm{T}}[\mathbf{F}(\mathbf{t}_{\mathrm{d}} + \mu\mathbf{t}_{\mathrm{l}}) - \mathbf{H}\bar{\mathbf{u}}] + \mathbf{R}^{\mathrm{T}}\mathbf{G}_{\sigma}^{\mathrm{T}}\nabla_{\sigma}(\mathbf{Q}\cdot\Lambda + \tfrac{1}{2}\alpha\mathbf{Q}\cdot\mathbf{Q}) = \mathbf{0},$$

$$\mathbf{R}^{\mathrm{T}}[\mathbf{F}\mathbf{R}\,\mathbf{s}_0 + \mathbf{F}(\mathbf{t}_{\mathrm{d}} + \mu\mathbf{t}_{\mathrm{l}}) - \mathbf{H}\bar{\mathbf{u}} + \mathbf{G}_{\sigma}^{\mathrm{T}}\nabla_{\sigma}(\mathbf{Q}\cdot\Lambda + \tfrac{1}{2}\alpha\mathbf{Q}\cdot\mathbf{Q})] = \mathbf{0},$$

$$\mathbf{R}^{\mathrm{T}}[\mathbf{F}\mathbf{s} - \mathbf{H}\bar{\mathbf{u}} + \mathbf{G}_{\sigma}^{\mathrm{T}}\nabla_{\sigma}(\mathbf{Q}\cdot\Lambda + \tfrac{1}{2}\alpha\mathbf{Q}\cdot\mathbf{Q})] = \mathbf{0}. \tag{117}$$

The last equation, introducing definitions (109) (111) is identical to (116).

3.6. Augmented Lagrangian iteration

The core of the augmented Lagrangian method (ALM) is to allow for distinct iterations on direct and dual variables. When iteration is made on a set of variables the others are considered to be constant according to the general iterative scheme

$$\mathbf{s}_{0_{k+1}} = U_{s_0}(\Lambda_{k+1}, \mathbf{s}_0), \tag{118}$$

$$\Lambda_{k+1} = U_{\Lambda}(\Lambda, \mathbf{s}_{0_k}, \alpha_k), \tag{119}$$

$$\alpha_{k+1} = U_{\alpha}(\Lambda_{k+1}, \mathbf{s}_{0_{k+1}}, \alpha_k), \tag{120}$$

where U_{s_0}, U_{Λ}, U_{α}, respectively, are called the Lagrangian multiplier update formula, the direct variable update formula and the penalty parameter increment scheme. Eqs. (118) (120) are evaluated in sequence until convergence on the direct and dual variables is achieved. One of the most widely used versions of the augmented Lagrangian iteration (118) (120) is the Hestenes [24] and Powell [25] form. This has been adopted in the present work and iterates as follows:

$$\mathbf{s}_{0_{k+1}} = \arg\min_{\mathbf{s}_0} \Pi_{\mathrm{C}}^{\mathrm{al}}(\mathbf{s}_0, \Lambda_k), \tag{121}$$

$$\Lambda_{k+1} = \Lambda_k + \alpha_k\mathbf{Q}(\mathbf{s}_{0_{k+1}}), \tag{122}$$

$$\alpha_{k+1} = U_{\alpha}(\Lambda_{k+1}, \mathbf{s}_{0_{k+1}}, \alpha_k). \tag{123}$$

Given initial values for the multipliers Λ and the penalty parameter α, Eq. (122) is equivalent to a steepest-ascent iteration with a stepsize equal to α, [18] while the minimisation w.r.t. the self-equilibrated stresses is implemented using the Newton method. Formula (122) is known as the Hestenes Powell update formula. Finally, the penalty parameter is incremented as follows, modifying the classical scheme reported in Fletcher [26],

$$\alpha_{k+1} = \begin{cases} 10\alpha_k & \text{if } \left\|\mathbf{Q}(\mathbf{s}_{0_{k+1}})\right\| < \left\|\mathbf{Q}(\mathbf{s}_{0_k})\right\| \text{ and } \left\|\mathbf{Q}(\mathbf{s}_{0_{k+1}})\right\| > 0.25\left\|\mathbf{Q}(\mathbf{s}_{0_k})\right\|, \\ \alpha_k & \text{otherwise} \end{cases} \tag{124}$$

that is, the penalty parameter is increased by an order of magnitude if the norm of the constraint functions between two subsequent iterations decreases but does not decrease "sufficiently". The first condition has been introduced because, if some numerical instability arises, incrementing the penalty parameter causes nonconvergence even if convergence could be achieved. The penalty parameter increment scheme is of fundamental importance when the Hestenes Powell formula is used and its optimal value is not known. In fact, the magnitude of the penalty parameter strongly affects both the rate of convergence on the Lagrangian multipliers [18] and the conditioning of the direct problem. In this sense the scheme (124) determines an optimal value to satisfy both requisites and it can be shown that the sequence $\{\alpha_k\}$ generated by (124) is bounded whenever the multiplier values at the solution are bounded.

In the present work maximum principal stress regularisation of the indicator functional has been used in order to obtain a strictly convex minimisation problem in the direct step (121) of the iteration. In this case,

in fact, the only nonconvex term of the functional $\Pi_C^{al}(\mathbf{s}_0)$ is the square of the constraint functions $(1/2)\alpha\mathbf{Q}\cdot\mathbf{Q}$ (see Table 1) but, provided that the first iteration w.r.t the variables $\mathbf{s}_0$, Eq. (121), is made with the values of the multipliers equal to zero ($\Lambda = \mathbf{0}$), the augmented Lagrangian iteration generates a sequence of points $\{\mathbf{s}_{0_k}\}$ where the Hessian of the term $(1/2)\alpha\mathbf{Q}\cdot\mathbf{Q}$ is always positive definite. The same result does not hold if stress invariant regularisation is used, as is shown below:

Consider, for the sake of simplicity, the scalar constraint function $\sigma_M^+ = \max(\sigma_M, -\lambda/\alpha)$. The Hessian of σ_M^2 is

$$\nabla^2(\sigma_M^2) = \begin{cases} 2\sigma_M\nabla^2\sigma_M & \text{if } \sigma_M \geqslant -\lambda/\alpha, \\ \mathbf{0} & \text{otherwise.} \end{cases} \tag{125}$$

As $\nabla^2\sigma_M$ is positive semidefinite ($\mathscr{K}_\sigma$ being a cone) $\nabla^2(\sigma_M^2)$ is negative definite whenever $\sigma_M < 0$ and $-\lambda/\alpha \leqslant \sigma_M < 0$, that is, when $\lambda \geqslant -\alpha\sigma_M > 0$. The Hestenes and Powell update formula in this particular case is given by

$$\lambda_{k+1} = \lambda_k + \alpha \max(\sigma_M(\mathbf{s}_{0_k}), -\lambda_k/\alpha_k) \tag{126}$$

and therefore if the initial value of λ is zero $\lambda > 0$ can only hold if $\sigma_M > 0$. If during the iterations $\sigma_M < 0$ (i.e. the constraint becomes inactive), Eq. (126) immediately sets $\lambda = 0$ so that $\nabla^2(\sigma_M^2)$ is always positive definite whenever the constraint is active.In the numerical implementation of the augmented Lagrangian algorithm step (121) has been realised by a pure Newton scheme and presents high rates of convergence. The nonexistence of the solution because of load incompatibility is revealed by an oscillation of the Newton iteration between two fixed points.

4. Numerical examples

In this section the proposed approach is applied to some two-dimensional tests in order to assess its effectiveness. The examples have been selected in order to explore the ability of the model to simulate the various aspects of no-tension material behaviour, and particularly the continuity/discontinuity of the solution and the problem of limit load determination. The results of these tests are of course not exhaustive, and their intent is to show the main features of the computational model. Therefore the following four solution typologies have been considered:

- continuous stresses and displacements;
- discontinuous displacements and stresses;
- continuous stresses and discontinuous displacements;
- limit load evaluation.

For the first three cases, examples for which the exact solution is known have been used for comparison; in the last case the collapse multiplier has also been determined by means of classical limit analysis.

The analyses have been carried out using a four-node isoparametric element with linear interpolation functions on both the displacements and the stresses. A control point for the admissibility constraint located at the centre of each element has been considered. Therefore, at the solution the principal stress tensor is always negative semidefinite at the centre of each element, while tractions can be observed at the corners. It should be noted, however, that the analytical and graphical results presented in the following subsections have not been filtered (as is usually done in common finite element restitutions) in order to provide the reader with the detailed solution properties.

4.1. Anular section with internal external pressure

An anular tube with an internal radius of $r_i = 0.2$ m and an external radius of $r_e = 1.0$ m, subjected to an internal pressure of $p_i = 1.0$ MPa and an external one of $p_e = 0.22$ MPa was analysed. The exact solution of the problem was given by Bennati and Padovani [27] and is used here for comparison. Moreover, considering the axial symmetry of the problem, a quarter of the tube was discretised and the following values for the elastic constants were assumed: $E = 10^4$ MPa, $\nu = 0.1$. The discretisation was made using 10 elements in the hoop direction, and four meshes were analysed, with 8, 10, 16, 25 elements in the radial

direction. Fig. 3 shows the mesh in the case of 16 elements in the radial direction, for a total of 160 elements. The mesh is constrained for horizontal displacements along the vertical edge and for vertical displacements along the horizontal one. The dimension of the self-equilibrated stress vector $\mathbf{s}_0$ (i.e. the number of direct variables) for the discretisations examined is equal to 117, 143, 221, 338 while one Lagrangian multiplier for each element of the mesh has to be controlled.

In Figs. 4 6 the computed displacements and stresses are plotted vs. the exact ones. The results for the radial stress and displacements are very close for any of the discretisations used. The hoop stress presents an oscillatory behaviour about the zero value in the inner part, where the solid presents the cracked zone and the stress admissibility constraint is active. As noticed before, this is due to the fact that the no-tension constraint is enforced at the element centres and can be violated elsewhere, due to linear variation in the stress field. This drawback can be removed by developing suitable filtering techniques for the solution. In

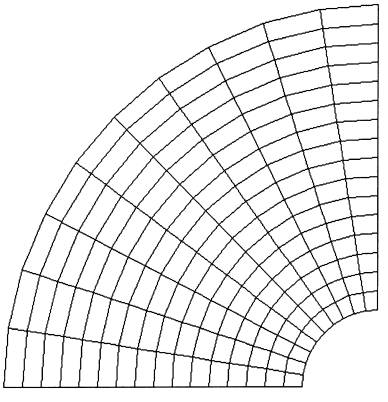

Fig. 3. Discretisation of the anular tube problem with 16 radial elements.

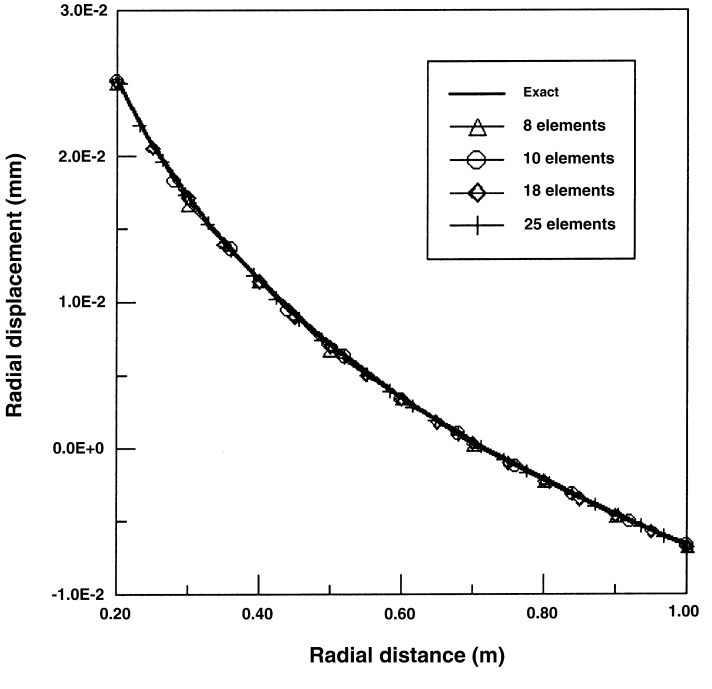

Fig. 4. Radial displacements for the anular tube problem.

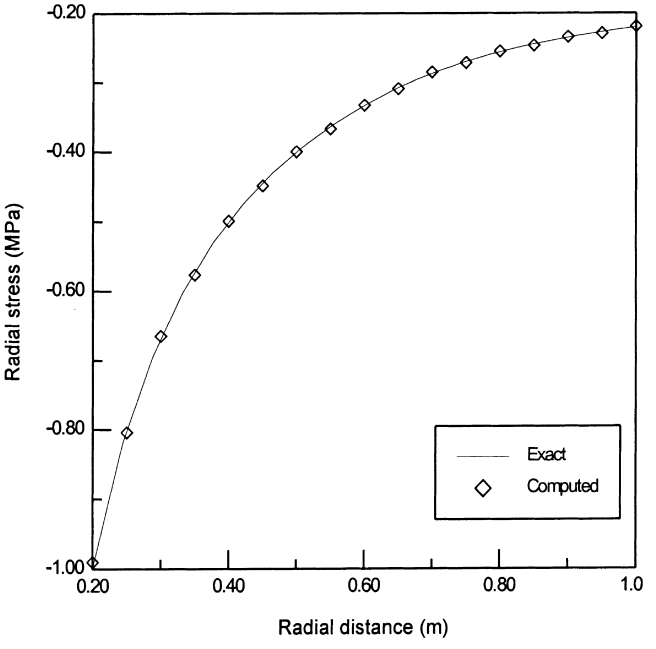

Fig. 5. Radial stress for the anular tube problem.

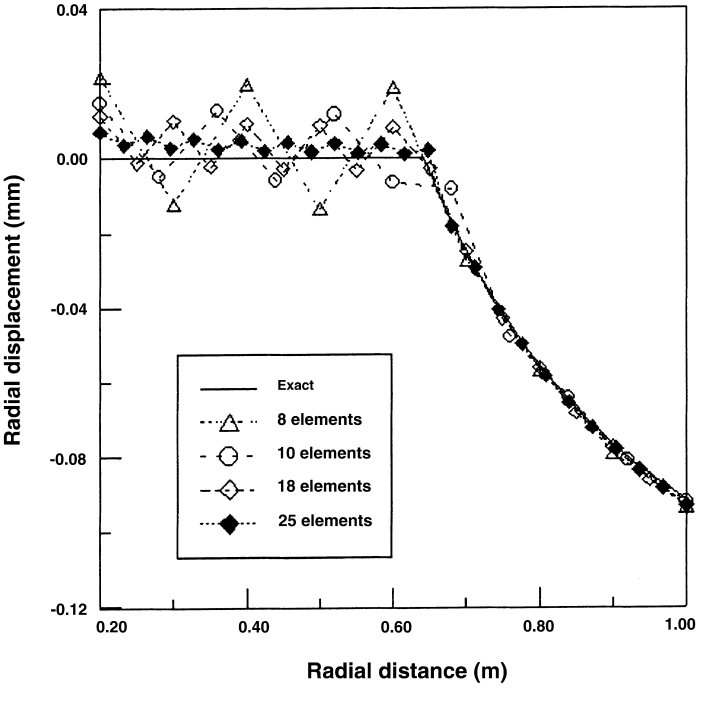

Fig. 6. Hoop stress for the anular tube problem.

fact, the oscillatory behaviour of the solution decreases when more elements in the radial direction are used. Moreover, it must be noted that the results presented refer to the nodes placed on the horizontal edge of the meshes, and not to a line through the Gauss points of the elements. For this reason the solution shown in Fig. 6 is characterised by small tensile stresses in the inner part of the anular tube and does not have zero crossings.

The oscillations near the zero value and the expected polar symmetry of the solution can also be observed from the contour plots of the stresses, Figs. 7 and 8, relating to the 16 radial element case.

4.2. Vertically loaded panels

The behaviour of the proposed approach in approximation of the discontinuous field is illustrated here with the aid of two examples: (a) a homogeneous square panel vertically loaded by two uniform loads of different intensity, Fig. 9, and (b) a two-material panel with a uniform vertical load, Fig. 10. These two examples were analysed using a mesh of 16×8 elements in the horizontal and vertical direction, respectively. The mesh has 153 nodes, while the number of direct variables is equal to 171.

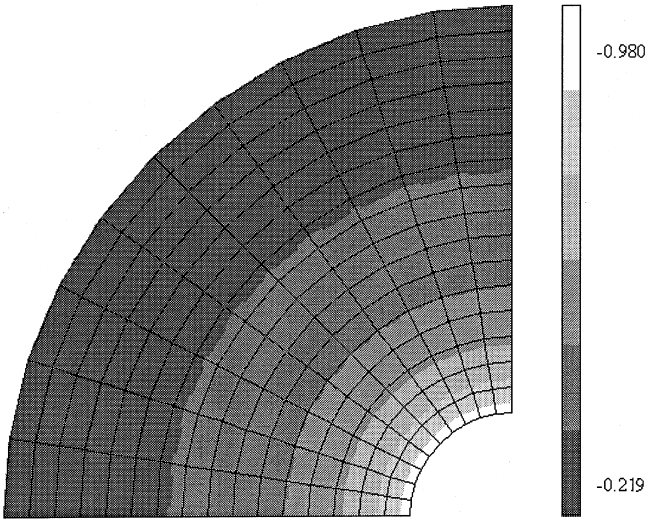

Fig. 7. Contours of the radial stress for the anular tube problem.

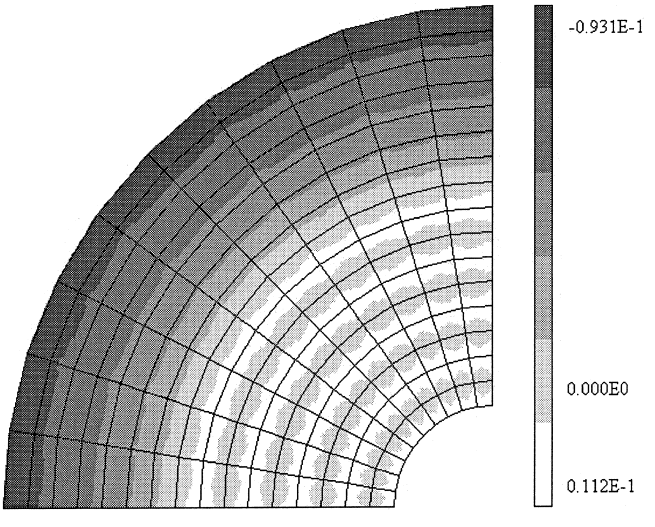

Fig. 8. Contours of the hoop stress for the anular tube problem.

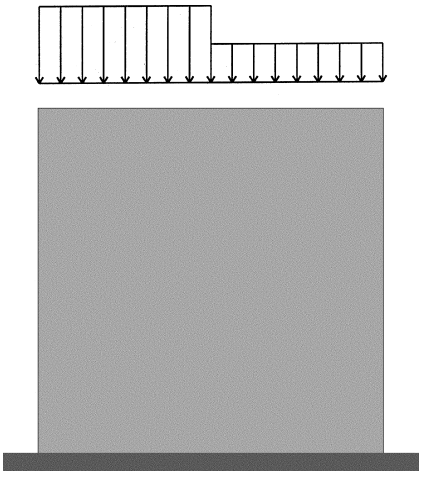

Fig. 9. Homogeneous panel with nonuniform load (a).

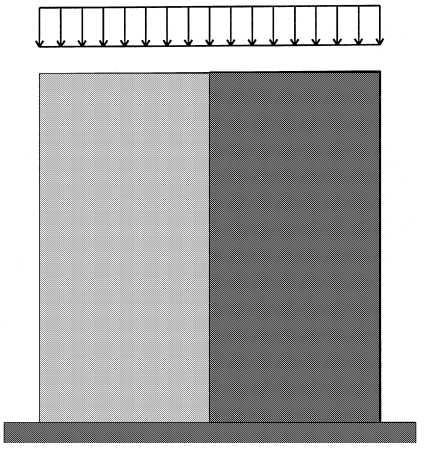

Fig. 10. Two material panel with uniform load (b).

In example (a) the elastic constants were set to $E = 5.0\ 10^3$ MPa, and $v = 0.0$ and the vertical loads have the values $p_1 = 0.2$ MPa, and $p_2 = 0.1$ MPa. The exact solution is characterised by the independent uniaxial behaviour of the two halves of the panel, and a comparison with the computed and linear elastic solutions is shown in Figs. 11 and 12.

The no-tension solution is very close to the exact one and is almost constant at every section. Similar behaviour is observed for the top panel displacements, Fig. 12. Here the elastic solution is smoothed all over the width of the panel while the no-tension solution approximates the discontinuous solution far better.

Example (b), Fig. 10, is characterised by a continuous (and constant) vertical stress and a discontinuous displacement field. The problem data are a vertical load of $p = 0.1$ MPa, and the elastic constants $E_1 = 1.0\ 10^4$ MPa, $v_1 = 0.0$ for the left part and $E_2 = 5.0\ 10^3$ MPa, $v_2 = 0.0$ for the right part.

The computed solution for the vertical stress at midheight shows an almost constant stress for the no-tension model, while the linear elastic solution presents sharp oscillations near the material discontinuity, Fig. 13.

The top vertical displacement, Fig. 14, follows the same qualitative behaviour described for example (a), Fig. 12.

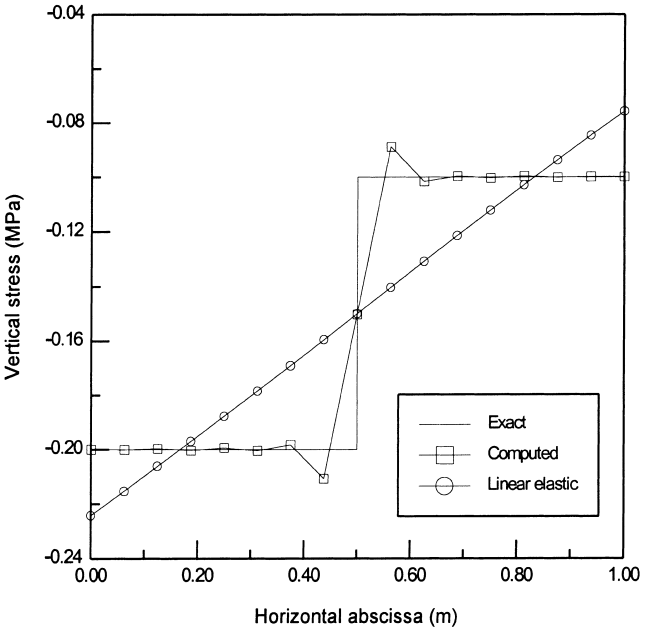

Fig. 11. Vertical stress for example (a) at the bottom of the panel.

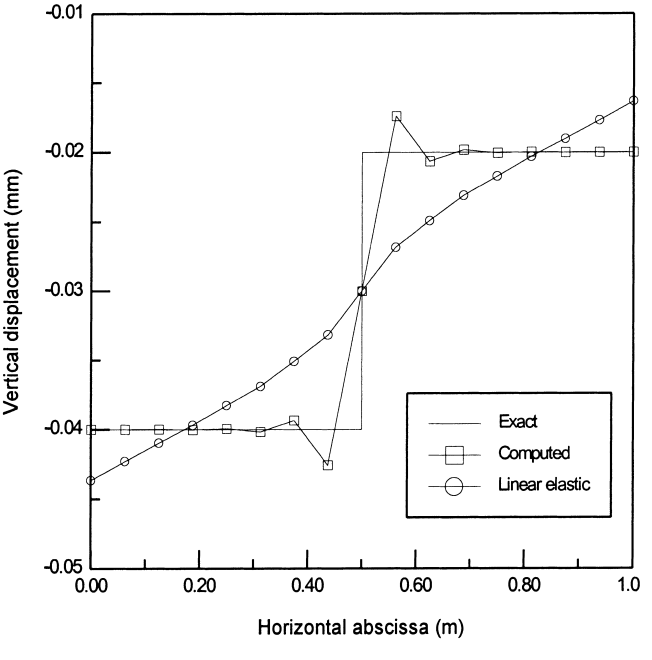

Fig. 12. Top vertical displacement for example (a).

4.3. Circular arch with lateral force

The problem of determining the limit load has been solved for a circular arch subjected to an external hydrostatic pressure $p_e = 0.1$ MPa and a horizontal force F, as illustrated in Fig. 15, where the deformed geometry immediately before collapse is also shown.

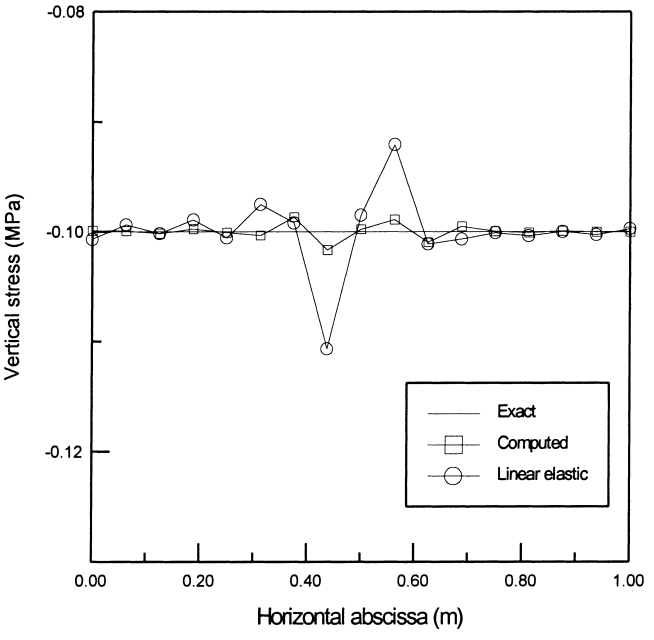

Fig. 13. Vertical stress for panel (b).

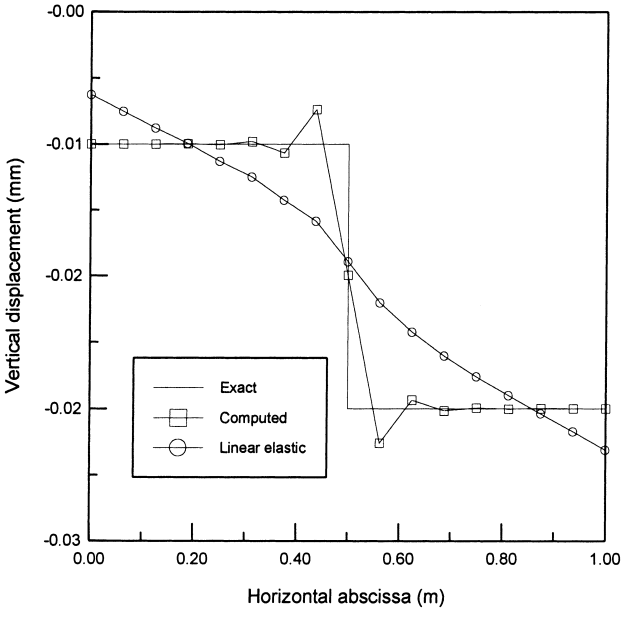

Fig. 14. Top vertical displacement for panel (b).

The arch is characterised by an internal radius r_i of 0.4 m, an external radius r_e of 0.5 m, a thickness $r_e - r_i$ of 0.1 m and the elastic constants $E = 10^4$ MPa, $v = 0.1$. It was discretised using 80 elements and 105 nodes, for a total of 121 direct variables. The load displacement curve was constructed until convergence was lost and is shown in Fig. 16.

The last convergent step of the program was obtained for a value of $F = 0.215$ KN, and is, of course, independent from the value of the elastic constants (apart from excessively high and low values introducing numerical ill conditioning). The computed limit load can be compared to the one obtained by classical limit

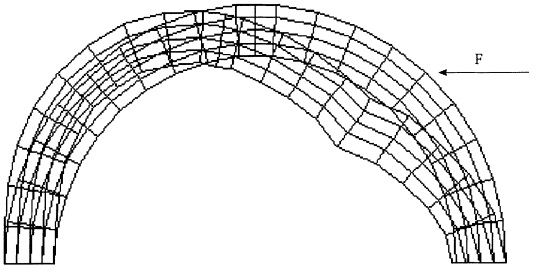

Fig. 15. Undeformed and deformed geometry for the circular arch problem.

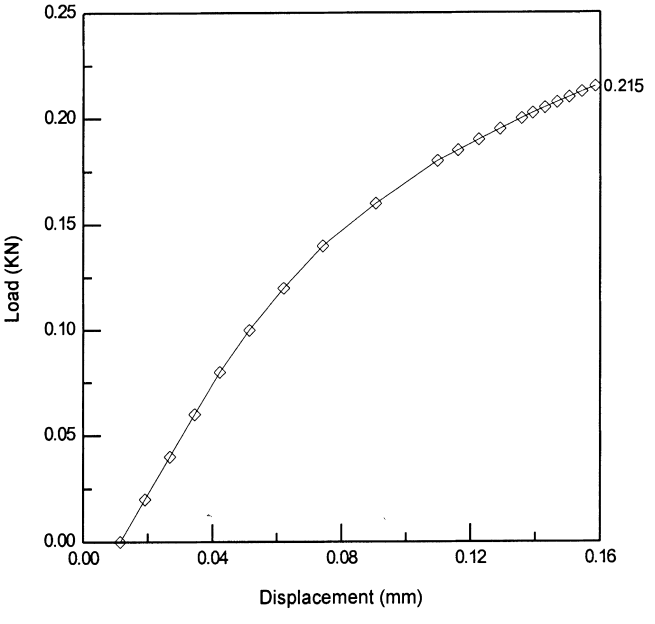

Fig. 16. Load displacement curve for the circular arch problem.

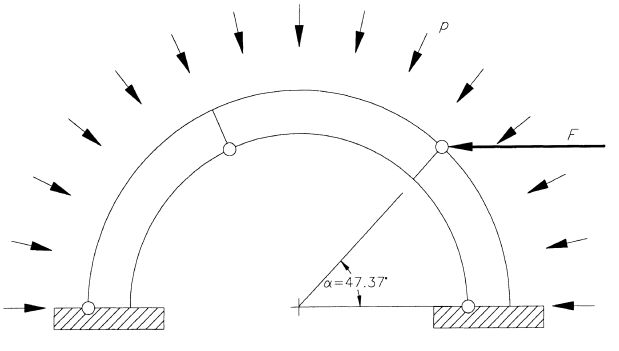

Fig. 17. Limit load problem for the circular arch.

load analysis, carried out by the lower bound theorem assuming the collapse mechanism of Fig. 17 with three fixed hinges and determining the fourth by minimising the collapse multiplier. Of course, since the program enforces the admissibility constraint at the centres of the elements, the thickness of the arch to be used to determine the collapse load must be set accordingly, i.e. $t = r_e - r_i - (r_e - r_i)/4$, 4 being the number

of finite elements along the thickness. In this way, a limit load of $F = 0.272$ KN was determined, which is comparable to the value computed by the no-tension model.

5. Conclusions

A computational formulation for the problem of no-tension solids based on CE has been presented. Similar approaches have been previously proposed in literature. However these methods, as well as those based on displacement formulations, have a particularly slow rate of convergence and are sometimes numerically unstable. The proposed method differs from previous ones both in the variational formulation and in the finite element implementation. The functionals stemming from the variational formulation have been regularised using the augmented Lagrangian technique, obtaining a continuous and differentiable functional. From the continuum variational formulation a complementary finite element form of the problem has been developed, where the equilibrium equations are imposed in a weak sense and the constraint multipliers are determined using augmented Lagrangian algorithms. This has allowed the discretised problem in nodal self-equilibrated stresses to be restated as primal (direct) variables. A particularly efficient and stable solution scheme based on alternate iteration over the direct variables and the Lagrangian multipliers is obtained. In particular, it has been demonstrated that regularisation based on the maximum principal stress has the property of generating in the augmented Lagrangian iteration a sequence of points for which the direct and dual problems are, respectively, strictly convex and concave (provided that a solution exists), and is therefore particularly suitable for numerical applications.

The numerical efficiency of the algorithm, in the formulation presented , is strongly influenced by certain factors: the Hessian of the complementary energy functional generally has a sparse structure, so that its inversion is time consuming. Although the first-order Lagrangian multiplier update formula (122) by Hestenes and Powell is computationally very convenient, it presents a linear convergence rate. Further analysis of the numerical aspects of the problem, as well as improvements to the present scheme, will be presented in a forthcoming paper.

References

[1] F. Genna, M. Di Pasqua, Numerical analysis of masonry structures: a comparison between 'no tension' and 'softening' costitutive laws, in: Proceedings of VII National Conference for Computational Mechanics, Trieste, 1993, pp. 212 217.
[2] L. Gambarotta, S. Lagomarsino, A microcrack damage model for brittle materials, Int. J. Solids Structures 30 (2) (1993) 177 198.
[3] C.A.P. Castigliano, Theorie de l'Equilibre des Systemes Elastiques et ses Applications, Augusto Federico Negro, Torino, 1879.
[4] J. Heyman, The stone skeleton, Int. J. Solids and Structures 2 (1966) 249 279.
[5] E. Sacco, Modellazione e calcolo di strutture in materiale non reagente a trazione, Rend. Mat. Acc. Lincei, s.9, v.1 (1990) 235 258.
[6] G. Romano, E. Sacco, Sul calcolo di strutture non resistenti a trazione, in: Proceedings of VII AIMETA National Congress Trieste, Italy, 1984, V, pp. 217 226.
[7] M. Lucchesi, C. Padovani, G. Pasquinelli, On the numerical solution of equilibrium problems for elastic solids with bounded tensile strength, Comput. Methods Appl. Mech. Engrg. 127 (1995) 37 56.
[8] F. Genna, An accurate numerical integration scheme for solving structural problems in the presence of a ''no tension'' material, Computers and Structures 53 (1994) 253 273.
[9] G. Maier, A. Nappi, A theory of no tension discretized structural systems, Eng. Struct. 12 (1990) 227 234.
[10] A. Grimaldi, E. Sacco, Energia complementare e metodo penalty per problemi elastici unilaterali, in: Proceedings of IX AIMETA National Congress, Bari, Italy, 1988, pp. 615 618.
[11] A. Curnier, Q.C. He, P. Zysset, Conewise linear elastic materials, J. Elasticity 37 (1995) 1 38.
[12] G. Anzelotti, Elasticity with unilateral constraints on the stress, in: Proceedings International workshop on Integral Functionals in Calculus of Variations, Suppl. Rend. Circolo Matematico di Palermo s.2 (15), 1987, pp. 135 141.
[13] M. Giaquinta, E. Giusti, Researches on the equilibrium of masonry structures, Arch. Rat. Mech. Anal. 68 (1985) 359 392.
[14] G. Del Piero, Recent developments in the mechanics of materials which do not support tension, International report IMTA/056, University of Udine, Italy, 1988.
[15] G. Del Piero, A generalized Gauss Green formula for the Mathematical Theory of Plasticity, in: Proceedings of the Icclem Conference, Chongqing, China, 1989.
[16] S. Di Pasquale, Statica dei solidi murari: teorie ed esperienze, Internal report, University of Firenze, Dipartimento di Costruzioni, Firenze, 1984.
[17] G. Del Piero, Constitutive equation and compatibility of the external loads for linear elastic masonry like materials, Meccanica 24 (1989) 150 162.

[18] D.P. Bertsekas, Constrained Optimization and Lagrange Multiplier Methods, Academic Press, San Diego, CA, 1982.
[19] N. Kikuchi, J.T. Oden, Contact Problems in Elasticity: A Study of Variational Inequalities and Finite Element Methods, SIAM, Philadelhia, 1988.
[20] J.H. Heegard, A. Curnier, An augmented Lagrangian method for discrete large-slip contact problems, Int. J. Numer. Methods Engrg. 36 (1993) 569–593.
[21] M. Cuomo, G. Ventura, Complementary energy approach to contact problems based on consistent augmented Lagrangian formulation, Math. Comput. Modelling 28 (4–8) (1998) 185–204.
[22] M. Cuomo, G. Ventura, An effective computational implementation of the no-tension model for masonry structures, in: G.N. Pande, J. Middleton (Eds.), Proceedings of the Computer Methods in Structural Masonry, Books and Journals International LTD, Swansea, 1993.
[23] M. Cuomo, G. Ventura, An augmented Lagrangian formulation for the analysis of no-tension structures with unilateral supports, in: M Raous, M. Jean, J.J. Moreau (Eds.), Proceedings II Contact Mechanics International Symposium, Plenum Press, New York, London, 1995.
[24] M.R. Hestenes, Multiplier and gradient methods, J. Optim. Theory Appl. 4 (1969) 303–320.
[25] M.J.D. Powell, A method for non-linear constraint in optimization problems, in: R. Fletcher (Ed.), Optimization, Academic Press, London, 1969, pp. 283–298.
[26] R. Fletcher, Practical Methods of Optimization, Wiley, New York, 1987.
[27] S. Bennati, C. Padovani, Soluzioni esplicite per problemi di equilibrio di solidi non reagenti a trazione, in: The Proceedings of XI AIMETA National Congress, Solids and Structures Mechanics, Trento, Italy, 1992, pp. 73–78.